mathematics

MDPI

Article

Refined Green-Function Estimates for a Caputo Fractional Three-Point Boundary Value Problem: Sharper Existence, Uniqueness, and Ulam–Hyers Stability Conditions

Abdelhamid Taieb Zaidi

Department of Mathematics, College of Science, Qassim University, P.O. Box 6644, Buraydah 51452, Saudi Arabia; a.zaidi@qu.edu.sa

Abstract

We study a Caputo fractional three-point boundary value problem of order $\alpha \in (c-1, c]$ and establish three interrelated contributions, all resting on a single refined pointwise $\mathbf{L}^2$ estimate for the associated Green function $\mathbf{Gr}(t,s)$. First, we derive a tighter upper bound for $\sup_{0<t<1} \int_0^1 \mathbf{Gr}^2(t,s)\, ds$ by retaining a sign-definite negative mixed term that the classical $\mathbf{L}^1$-based analysis of Shivanian discards. The resulting admissible Lipschitz constant $\mathcal{K}_B$ is explicit in α, a, b, c and exceeds Shivanian's constant $\mathcal{K}_S$ under an explicit algebraic condition; a closed-form refinement $\mathcal{K}_B^* \geq \mathcal{K}_B$ follows by maximising the pointwise bound in closed form. On Shivanian's benchmark, the admissible constant rises from 14.646 to 23.220 and then to 32.165. Second, the same contraction constant yields an explicit Ulam–Hyers stability theorem for this problem. While a stability estimate already follows from the classical $\mathbf{L}^1$ condition, the refined constant both enlarges the range of admissible Lipschitz constants for which stability is certified and yields a strictly smaller stability constant. Third, we establish quantitative continuous-dependence bounds with respect to the nonlinearity h and the boundary parameter a, and characterize the deterioration of the contraction-based boundary-parameter estimate as the problem approaches resonance. For a fixed Lipschitz constant, this estimate becomes singular as the perturbed contraction factor approaches one and ceases to apply once the contraction condition fails. A more accurate analysis of the Green function thus simultaneously sharpens solvability conditions, stability estimates, and sensitivity bounds for nonlinear Caputo fractional boundary value problems.

Keywords: fractional derivative; three-point boundary value problem; Green function; Banach fixed-point theorem; existence and uniqueness; Ulam–Hyers stability; continuous dependence; nonlinear equations

MSC: 34A08; 47H10

Check for updates

Academic Editor: Jay M. Jahangiri

Received: 7 July 2026
Revised: 21 July 2026
Accepted: 22 July 2026
Published: 6 August 2026

1. Introduction

Fractional differential equations provide a powerful framework for modelling memory and hereditary effects in physical [1], biological [2,3], and engineering [4,5] systems, because the Caputo derivative encodes a weakly singular memory kernel that classical integer-order models cannot reproduce. The same non-local structure that makes these models expressive also makes their qualitative theory delicate: existence, uniqueness and stability hinge on fine estimates of the associated Green function, and coarse bounds translate directly into unnecessarily restrictive conditions on the nonlinearity. At the cellular and microbial scale, engineered feedback and selection mechanisms can likewise shape population-level dynamics [6]. Multi-point boundary conditions, in turn, arise whenever a state is constrained at interior locations—for instance in beam and thermostat models and in feedback designs that sample the solution away from the endpoints—so that three-point Caputo problems occupy a natural middle ground between initial-value and classical two-point theory. Boundary value problems involving Caputo derivatives are particularly important because Caputo derivatives allow the use of classical initial and boundary conditions. In this work, we consider the Caputo fractional three-point boundary value problem

$$\begin{cases} D_t^{\alpha} u(t) + h(t, u(t)) = 0, & t \in (0,1), \\ u(0) = u'(0) = \cdots = u^{(c-2)}(0) = 0, & u(1) = a\, u(b) \end{cases} \tag{1}$$

where D_t^{α} denotes the Caputo fractional derivative of order α and

$$c - 1 < \alpha \leq c, \qquad c \in \mathbb{N},\ c \geq 2, \qquad 0 < b < 1, \qquad a\, b^{c-1} \neq 1. \tag{2}$$

The condition $a\, b^{c-1} \neq 1$ in (2) is a *nonresonance* requirement, and admits a transparent interpretation. The homogeneous problem $D_t^{\alpha} u = 0$ subject to $u(0) = u'(0) = \cdots = u^{(c-2)}(0) = 0$ admits precisely the one-parameter family $u(t) = \gamma\, t^{c-1}$, $\gamma \in \mathbb{R}$. Evaluating the three-point functional on this family gives

$$u(1) - a\, u(b) = \gamma\big(1 - a\, b^{c-1}\big),$$

which vanishes for some $\gamma \neq 0$ exactly when $a\, b^{c-1} = 1$. On that locus, the boundary condition $u(1) = a\, u(b)$ is satisfied by a nontrivial solution of the homogeneous problem, so uniqueness for (1) fails; correspondingly the constant $D = (1 - ab^{c-1})^{-1}$ of (6), and with it the Green function, diverges. Geometrically, since $u(b)/u(1) = b^{c-1}$ for the homogeneous solution $u(t) = t^{c-1}$, the singular curve $a = b^{1-c}$ is precisely the locus on which the multiplier a exactly compensates the natural growth of t^{c-1} between $t = b$ and $t = 1$.

The existence and uniqueness of solutions to (1) were studied by Shivanian [7] using Banach's contraction principle and a uniform $\mathbf{L}^1$ estimate of the associated Green function. More precisely, if the nonlinear term h satisfies

$$|h(t,x) - h(t,y)| \leq \mathcal{K}|x - y|, \qquad t \in [0,1], \quad x, y \in \mathbb{R}, \tag{3}$$

then Shivanian's sufficient condition is

$$\mathcal{K} < \frac{\Gamma(\alpha+1)}{2\left(1 + \left|\dfrac{a}{1 - a\, b^{c-1}}\right|\right)}. \tag{4}$$

Fractional differential equations have become a standard tool for modelling memory and hereditary phenomena, and the foundations of the subject are documented in the monographs of Podlubny [8], Kilbas, Srivastava and Trujillo [9], and Diethelm [10]. Among the various fractional operators, the Caputo derivative is particularly convenient for boundary value problems because it admits initial and boundary conditions of classical type [9,10].

Multipoint and nonlocal boundary conditions, of which the three-point condition $u(1) = a\, u(b)$ in (1) is a prototype, go back to the work of Il'in and Moiseev [11] on nonlocal Sturm–Liouville problems and to Gupta [12], who initiated the systematic study of three-point conditions for nonlinear second-order equations. In the fractional setting, existence theory for two-point and multipoint boundary value problems developed rapidly after the work of Bai and Lü [13], who combined the Green-function formulation with fixed-point theorems on cones; subsequent contributions include [14,15], and a broad survey of fixed-point methods for fractional boundary value problems is given by Agarwal, Benchohra and Hamani [16]. High-order fractional problems with three-point conditions of the type (1) were considered by Chai and Hu [17] from the viewpoint of positive solutions, and more recently by Shivanian [7], who constructed the associated Green function explicitly, established the solvability criterion (4) via Banach's contraction principle [18], and applied the result to fractional optimal control.

A parallel line of research has shown that the admissible Lipschitz classes produced by contraction arguments depend critically on the accuracy of the underlying Green-function estimates. Smirnov [19] obtained existence and uniqueness results for third-order three-point problems via $\mathbf{L}^1$ bounds, and Almuthaybiri and Tisdell subsequently sharpened these results for third-order [20,21] and fourth-order [22] problems by combining refined integral estimates of the Green function, including $\mathbf{L}^2$ bounds used through the Cauchy–Schwarz inequality, with Banach's theorem and with Rus's fixed-point theorem involving two metrics [23]. These works demonstrate that more careful kernel analysis directly enlarges the class of nonlinearities for which existence and uniqueness can be guaranteed. To the best of our knowledge, however, this sharpening programme has not yet been carried out for the Caputo fractional three-point problem (1) of arbitrary order $\alpha \in (c-1, c]$, for which the only available Banach-type criterion remains the $\mathbf{L}^1$-based condition (4) of [7]. We stress from the outset that the present paper relies exclusively on Banach's contraction principle [18]; Rus's two-metric fixed-point theorem [23] is cited only to describe the methodology of [20–22] and is not used in our proofs.

Let us make the novelty with respect to [7] fully explicit. Shivanian's analysis bounds the kernel integral $\int_0^1 |\mathbf{Gr}(t,s)|\,ds$ by a uniform $\mathbf{L}^1$ estimate in which the three constituent terms of the Green function are majorised separately by their absolute values; all cancellation between them is lost. The present paper instead estimates $\int_0^1 \mathbf{Gr}^2(t,s)\,ds$ and feeds the result into the contraction argument through the Cauchy–Schwarz inequality. Squaring the kernel produces a *mixed term* $2[I_2(t) - I_1(t)]$ (see Lemma 2) which is sign-definite and negative in a large explicit parameter regime; retaining it, rather than discarding it, is precisely what enlarges the admissible Lipschitz class. The practical significance of the $\mathbf{L}^2$-based approach is therefore threefold: (a) it certifies existence and uniqueness for nonlinearities whose Lipschitz constants exceed Shivanian's threshold (on the benchmark problem the admissible constant increases by the factors 1.585 and 2.196); (b) the same sharper contraction constant q sharpens the Ulam–Hyers theory: a stability estimate already follows from Shivanian's $\mathbf{L}^1$ condition whenever $q_S < 1$, and the refined constant both widens the certified range and delivers the smaller (hence better) stability constant $(1-q)^{-1}$; and (c) it produces quantitative continuous-dependence bounds that are tighter than any bound the $\mathbf{L}^1$ estimate could deliver. All new constants remain fully explicit in α, a, b, c and are computable at negligible cost (Remark 15).

A further quality criterion for solutions of fractional differential equations is *Ulam–Hyers (UH) stability*, introduced in the functional-equation setting by Ulam [24] and Hyers [25] and subsequently extended to fractional boundary value problems by Wang, Lv and Zhou [26], Benchohra and Lazreg [27], and many others; see also the recent contributions [28,29] for UH stability of integer-order and fractional multipoint problems. UH stability asserts that approximate solutions remain close to exact solutions, a property of direct relevance to numerical computation and physical modelling. To date, and to the best of the author's knowledge, no explicit UH stability theorem has been stated for problem (1).

We are careful about what is and is not new here. An Ulam–Hyers estimate for (1) can already be obtained from the earlier $\mathbf{L}^1$-based contraction condition: whenever Shivanian's contraction factor satisfies $q_S < 1$, the same elementary argument as in Section 6 yields the stability constant $C^S_{\mathrm{UH}} = (1 - q_S)^{-1}$. The refined estimate is therefore not necessary for *proving* Ulam–Hyers stability; what it does is (i) enlarge the range of Lipschitz constants for which stability is certified, and (ii) produce a smaller, hence tighter, explicit stability constant.

More broadly, the field remains very active: among the most recent developments involving the Caputo operator and its generalisations, we mention the finite-difference/local discontinuous Galerkin analysis of fourth-order fractional diffusion–wave systems by Ran, Xu, Hou and Zhang [30], and the study of boundary value problems for systems of fractional differential equations with tempered Caputo derivatives [31].

Beyond classical modelling, fractional formulations are increasingly combined with data-driven and finite-volume solvers in the numerical treatment of transport phenomena—for instance in message-passing encoder–decoder architectures coupled to finite volume methods for water infiltration in unsaturated soils [32] and in physics-based, data-driven frameworks for the anomalous diffusion of water in soil [33]. These works are cited as broad computational context only: they concern different equations and different discretisations, and we make no claim that their convergence is governed by the Green-function constants developed here. They do, however, illustrate that fixed-point iterations are a standard ingredient in the numerical treatment of nonlinear and fractional models, which is one motivation for seeking sharp, computable contraction thresholds. Recent studies have likewise extended fractional and fractal modelling, together with dedicated numerical treatments, to N/MEMS devices, pendulum oscillators, and nonlinear wave systems [34–36].

The present paper addresses these three gaps simultaneously by exploiting a single refined $\mathbf{L}^2$ estimate of the Green function. The **main contributions** are as follows.

- **(i)** **Sharper existence and uniqueness (Sections 3–5).** We prove a tighter pointwise bound for $\sup_{0<t<1} \int_0^1 \mathbf{Gr}^2(t,s)\,ds$ by retaining a negative mixed term that the $\mathbf{L}^1$-based analysis of [7] discards. This yields an admissible Lipschitz constant $\mathcal{K}_B$ strictly larger than $\mathcal{K}_S$ in an explicit parameter regime, and a further closed-form refinement $\mathcal{K}_B^* \geq \mathcal{K}_B$.
- **(ii)** **Ulam–Hyers stability (Section 6).** Using the contraction constant furnished by the improved $\mathbf{L}^2$ estimate, we establish that every solution of (1) is Ulam–Hyers stable with an explicit, parameter-dependent stability constant. A stability estimate is already available from the classical $\mathbf{L}^1$ condition; the refined constant sharpens it, both enlarging the certified range and tightening the constant, and shows that the improved Green-function analysis has consequences beyond existence and uniqueness.
- **(iii)** **Continuous dependence on data (Section 7).** Using the contraction framework, we derive explicit quantitative bounds on how much the unique solution changes when the nonlinearity h (Theorem 5) or the boundary multiplier a (Proposition 2) is perturbed. The bounds are tighter than those obtainable from the $\mathbf{L}^1$-based analysis because the refined estimate yields a smaller contraction constant q. We further characterize the deterioration of the contraction-based sensitivity estimate as a approaches the singular regime $ab^{c-1} = 1$. For a fixed Lipschitz constant, the estimate becomes singular as $\tilde{q} \uparrow 1$ and ceases to apply once the contraction hypothesis fails.

In each case, the comparison is with the $\mathbf{L}^1$-based contraction framework of Shivanian [7]. The present contributions refine that framework by providing sharper explicit constants and by deriving quantitative Ulam–Hyers stability and continuous-dependence estimates from the improved contraction factor.

The paper is organised as follows. Section 2 recalls the fixed-point formulation and notation. Section 3 proves the improved Green-function estimate. Section 4 establishes the main Banach-type existence and uniqueness theorem. Section 5 compares the proposed condition with Shivanian's criterion. Section 6 establishes Ulam–Hyers stability. Section 7 derives continuous-dependence results, illustrates them numerically, and presents the full numerical study of admissible Lipschitz constants. Section 8 concludes the paper.

2. Preliminaries

Let $C([0,1])$ be the Banach space of continuous real-valued functions on $[0,1]$, endowed with the supremum norm

$$\|u\|_\infty = \max_{t\in[0,1]} |u(t)|.$$

According to [7], the solution of (1) is equivalent to a fixed point of the integral operator

$$(Tu)(t) = \int_0^1 \mathbf{Gr}(t,s) h(s,u(s))\, ds, \tag{5}$$

where $\mathbf{Gr}(t,s)$ is the Green function associated with problem (1).

For the reader's convenience, we collect in one place the standing assumptions used throughout the paper:

(H0) the structural conditions (2) hold, namely $c-1 < \alpha \le c$ with $c \in \mathbb{N}$, $c \ge 2$ (so that $n = \alpha - 1 > 0$), $0 < b < 1$, and $a\, b^{c-1} \ne 1$;

(H1) $h \in C([0,1]\times\mathbb{R},\mathbb{R})$;

(H2) h satisfies the global Lipschitz condition (3) in its second variable, uniformly in t, with constant $\mathcal{K}$.

Assumptions (H0)–(H1) are in force in all statements below; (H2) is invoked explicitly wherever a Lipschitz constant appears. Table 1 collects the notation used throughout the paper.

Table 1. Main notation.

Symbol	Meaning	Symbol	Meaning
α	fractional order, $\alpha \in (c-1, c]$	$Q(b,n)$	quadratic kernel integral (10)
c	integer ceiling of α, $c \ge 2$	$I(t)$	$\int_0^1 F^2(t,s)\,ds$, see (13)
m	$c-1$	I_1, I_2	mixed-term integrals (16), (17)
n	$\alpha - 1 > 0$	$\mathcal{K}$	Lipschitz constant of h, see (H2)
a, b	boundary data in $u(1) = a\,u(b)$	$\mathcal{K}_S$, $\mathcal{K}_B$, $\mathcal{K}_B^*$	admissible constants (29), (30), (28)
D, E	$\frac{1}{1-ab^m}$, $\frac{a}{1-ab^m}$, see (6)	δ, τ, $G(\delta)$	quantities of Corollary 1
$\mathbf{Gr}$, F	Green function and its kernel (7)	q, q^*, $\tilde{q}$	contraction constants (34)
$P(x,n)$	kernel integral (9)	σ, C_{UH}	perturbation size (36); UH constant (35)

Notational conventions. Throughout, the Green function is denoted uniformly by $\mathbf{Gr}(t,s)$, and the admissible constants by $\mathcal{K}_S$, $\mathcal{K}_B$ and $\mathcal{K}_B^*$, with the superscript placed as in $\mathcal{K}_B^*$ and C_{UH}^B. We write $\sup_{0<t<1}$ for suprema of the kernel quantities I, Φ and $\int_0^1 \mathbf{Gr}^2(t,s)\,ds$ over the open interval $(0,1)$ on which problem (1) is posed, and $\sup_{t\in[0,1]}$ for suprema of continuous functions on the closed interval, such as norms in $C([0,1])$. The two agree for every quantity considered here, since each extends continuously from $(0,1)$ to $[0,1]$ (cf. Theorem 1); the distinction is kept only to indicate which interval is intrinsic to the object at hand.

Set $m = c-1$, $n = \alpha - 1$, and define

$$D = \frac{1}{1-ab^m}, \qquad E = \frac{a}{1-ab^m}. \tag{6}$$

The Green function given in ([7], Equation (14)) can be written as

$$\mathbf{Gr}(t,s) = \frac{1}{\Gamma(\alpha)} F(t,s), \tag{7}$$

where

$$F(t,s) = Dt^m(1-s)^n - (t-s)_+^n - Et^m(b-s)_+^n \quad \text{and} \quad (x)_+^n = \begin{cases} x^n, & x > 0, \\ 0, & x \leq 0. \end{cases} \tag{8}$$

Remark 1 (Continuity and boundedness of the Green function)**.** *Under (H0) one has $n > 0$, so each of the three terms in (8) is continuous on the square $[0,1]^2$ (the truncated powers $(t-s)_+^n$ and $(b-s)_+^n$ are continuous because $n > 0$). Hence F, and therefore $\mathbf{Gr} = F/\Gamma(\alpha)$, is continuous and bounded on $[0,1]^2$, with the crude uniform bound $|\mathbf{Gr}(t,s)| \leq \big(|D| + 1 + |E|\big)/\Gamma(\alpha)$. In particular, for every $u \in C([0,1])$ and h satisfying (H1), the integral operator T in (5) is well defined and maps $C([0,1])$ into itself; these are the continuity and boundedness properties used, without further comment, in all fixed-point arguments below.*

Lemma 1. *Let*

$$P(b,n) = \int_0^b (1-s)^n (b-s)^n \, ds, \tag{9}$$

$$Q(b,n) = \int_0^1 \left[D(1-s)^n - E(b-s)_+^n\right]^2 ds. \tag{10}$$

Then,

$$P(b,n) = \frac{b^{n+1}}{n+1} \, {}_2F_1(-n,1;n+2;b), \tag{11}$$

$$Q(b,n) = \frac{D^2 + E^2 b^{2n+1}}{2n+1} - 2D\,E\,P(b,n) > 0. \tag{12}$$

Proof. We prove identities (11) and (12) successively.

Before applying Euler's representation we verify absolute convergence explicitly, the endpoints $s \to 0^+$ and $s \to b^-$ being the only candidates for singular behaviour. In $P(b,n) = \int_0^b (1-s)^n (b-s)^n \, ds$ both exponents are positive, since $n = \alpha - 1 > 0$ by (H0); hence no endpoint singularity arises. Indeed the integrand tends to b^n as $s \to 0^+$ and to 0 as $s \to b^-$, and it is continuous and bounded on the compact interval $[0,b]$ by $\sup_{0 \leq s \leq b} (1-s)^n (b-s)^n \leq b^n$, so the integral converges absolutely as a proper Riemann integral. After the substitution $s = bu$, the transformed integrand $u \mapsto (1-bu)^n (1-u)^n$ is continuous on $[0,1]$, equals 1 at $u = 0$ and 0 at $u = 1$, and satisfies $1 - bu \in [1-b, 1]$, which is bounded away from 0 because $0 < b < 1$; consequently no negative power is ever evaluated at a zero of its argument. Finally, the parameter constraint $\mathfrak{Re}(r) > \mathfrak{Re}(q) > 0$ of Euler's formula reads $n + 2 > 1 > 0$, i.e., $n + 1 > 0$, which holds under (H0). Euler's integral representation therefore applies and both integrals converge absolutely.

1. Using the substitution $s = bu$, we obtain

$$P(b,n) = b^{n+1} \int_0^1 (1-bu)^n (1-u)^n \, du.$$

Applying Euler's integral representation of the Gauss hypergeometric function, written with dummy parameters p, q, r to avoid any clash with the fixed problem parameters a, b, c,

$${}_2F_1(p,q;r;z) = \frac{\Gamma(r)}{\Gamma(q)\Gamma(r-q)} \int_0^1 t^{q-1} (1-t)^{r-q-1} (1-zt)^{-p} \, dt,$$

which is valid whenever $\mathfrak{Re}(r) > \mathfrak{Re}(q) > 0$ and $|z| < 1$ (see, e.g., [9] or any standard reference on special functions), with $p = -n$, $q = 1$, $r = n + 2$, and $z = b$ (so that

$r - q = n + 1 > 0$ by (H0), and $0 < z = b < 1$; the integrand $(1 - bu)^n(1 - u)^n$ is continuous on $[0, 1]$, so the integral converges absolutely), yields

$$\int_0^1 (1 - bu)^n (1 - u)^n \, du = \frac{1}{n+1} {}_2F_1(-n, 1; n+2; b).$$

Consequently,

$$P(b, n) = \frac{b^{n+1}}{n+1} {}_2F_1(-n, 1; n+2; b).$$

2. Indeed, expanding the square in (10) gives

$$Q(b, n) = \int_0^1 \Big[D^2(1 - s)^{2n} - 2D\,E(1 - s)^n (b - s)_+^n + E^2(b - s)_+^{2n} \Big] ds.$$

Hence

$$Q(b, n) = D^2 \int_0^1 (1 - s)^{2n} ds + E^2 \int_0^1 (b - s)_+^{2n} ds - 2D\,E \int_0^1 (1 - s)^n (b - s)_+^n ds.$$

Now,

$$\int_0^1 (1 - s)^{2n} ds = \frac{1}{2n+1},$$

and since $(b - s)_+ = 0$ for $s \geq b$,

$$\int_0^1 (b - s)_+^{2n} ds = \int_0^b (b - s)^{2n} ds = \frac{b^{2n+1}}{2n+1}.$$

Moreover,

$$\int_0^1 (1 - s)^n (b - s)_+^n ds = \int_0^b (1 - s)^n (b - s)^n ds = P(b, n).$$

Therefore,

$$Q(b, n) = \frac{D^2}{2n+1} + \frac{E^2 b^{2n+1}}{2n+1} - 2D\,E\,P(b, n),$$

which is exactly

$$Q(b, n) = \frac{D^2 + E^2 b^{2n+1}}{2n+1} - 2D\,E\,P(b, n).$$

Finally, (10) shows that $Q(b, n) \geq 0$, since the integrand is a square. We now exclude every possible equality case. Suppose $Q(b, n) = 0$. The integrand $\psi(s) = \big[D(1 - s)^n - E(b - s)_+^n\big]^2$ is continuous and nonnegative on $[0, 1]$; a continuous nonnegative function with vanishing integral must vanish identically, so $\psi(s) = 0$ for *every* $s \in [0, 1]$, that is,

$$D(1 - s)^n = E(b - s)_+^n \quad \text{for all } s \in [0, 1].$$

However, fix any $s \in (b, 1)$: then $(b - s)_+ = 0$, so the right-hand side vanishes, while $D(1 - s)^n \neq 0$ since $D = (1 - ab^m)^{-1} \neq 0$ (recall $ab^m \neq 1$ by (H0)) and $1 - s > 0$. Thus no equality case can occur, for any admissible values of a, b, m, n. This contradiction proves that $Q(b, n) > 0$. □

Define

$$I(t) = \int_0^1 F^2(t, s)\, ds. \tag{13}$$

Then, by (7),

$$\int_0^1 \mathbf{Gr}^2(t, s)\, ds = \frac{1}{\Gamma(\alpha)^2} I(t). \tag{14}$$

Lemma 2. *For all $t \in (0,1)$, we have*

$$I(t) = Q(b,n)t^{2m} + \frac{t^{2n+1}}{2n+1} + 2[I_2(t) - I_1(t)], \tag{15}$$

where

$$I_1(t) = Dt^m \int_0^t (1-s)^n (t-s)^n \, ds \tag{16}$$

and

$$I_2(t) = Et^m \int_0^{\min(t,b)} (t-s)^n (b-s)^n \, ds. \tag{17}$$

Proof. For simplicity, write

$$J(t,s) = Dt^m(1-s)^n - Et^m(b-s)_+^n, \qquad K(t,s) = (t-s)_+^n.$$

Then $F(t,s) = J(t,s) - K(t,s)$ and, expanding the square of the difference term by term,

$$F^2(t,s) = \big(J(t,s) - K(t,s)\big)^2 = J^2(t,s) + K^2(t,s) - 2J(t,s)K(t,s).$$

Each of the three functions J^2, K^2 and JK is continuous in s on $[0,1]$ (Remark 1), so all the integrals below exist and integration may be carried out term by term. Therefore,

$$I(t) = \int_0^1 F^2(t,s)\, ds = \int_0^1 J^2(t,s)\, ds + \int_0^1 K^2(t,s)\, ds - 2\int_0^1 J(t,s)K(t,s)\, ds.$$

We now compute each term separately. First,

$$J(t,s) = t^m[D(1-s)^n - E(b-s)_+^n].$$

Thus,

$$\int_0^1 J^2(t,s)\, ds = t^{2m} \int_0^1 [D(1-s)^n - E(b-s)_+^n]^2 ds.$$

Using definition (10) of $Q(b,n)$, we have

$$\int_0^1 J^2(t,s)\, ds = Q(b,n)t^{2m}.$$

Next, since $K(t,s) = (t-s)_+^n$, we have

$$K(t,s) = \begin{cases} (t-s)^n, & 0 \le s \le t, \\ 0, & t < s \le 1. \end{cases}$$

Therefore,

$$\int_0^1 K^2(t,s)\, ds = \int_0^t (t-s)^{2n}\, ds.$$

Using the change of variable $u = t - s$, we obtain

$$\int_0^t (t-s)^{2n}\, ds = \int_0^t u^{2n}\, du = \frac{t^{2n+1}}{2n+1}.$$

It remains to compute the mixed term. Since

$$J(t,s)K(t,s) = [Dt^m(1-s)^n - Et^m(b-s)_+^n](t-s)_+^n,$$

we get

$$\int_0^1 J(t,s)K(t,s)\,ds = Dt^m \int_0^1 (1-s)^n (t-s)_+^n\,ds - Et^m \int_0^1 (b-s)_+^n (t-s)_+^n\,ds.$$

Because $(t-s)_+^n = 0$ for $s > t$, the first integral reduces to

$$\int_0^1 (1-s)^n (t-s)_+^n\,ds = \int_0^t (1-s)^n (t-s)^n\,ds.$$

Thus,

$$Dt^m \int_0^1 (1-s)^n (t-s)_+^n\,ds = I_1(t),$$

where $I_1(t)$ is given by (16).

Similarly, the product $(b-s)_+^n(t-s)_+^n$ is nonzero only when $s < b$ and $s < t$. Hence the domain of integration is $0 \le s \le \min(t,b)$. Therefore,

$$Et^m \int_0^1 (b-s)_+^n (t-s)_+^n\,ds = Et^m \int_0^{\min(t,b)} (b-s)^n (t-s)^n\,ds = I_2(t),$$

where $I_2(t)$ is given by (17). Consequently,

$$\int_0^1 J(t,s)K(t,s)\,ds = I_1(t) - I_2(t).$$

Substituting this into the expression for $I(t)$ gives

$$I(t) = Q(b,n)t^{2m} + \frac{t^{2n+1}}{2n+1} - 2(I_1(t) - I_2(t)).$$

Equivalently,

$$I(t) = Q(b,n)t^{2m} + \frac{t^{2n+1}}{2n+1} + 2(I_2(t) - I_1(t)),$$

which proves (15). □

3. Improved Green-Function Estimate

The decomposition (15) of Lemma 2 reduces the estimation of $I(t)$ to the control of the single mixed term $2[I_2(t) - I_1(t)]$: the first two terms of (15) are already explicit. The strategy of the next theorem is to compare the kernels of I_2 and I_1 through the elementary inequality $(b-s)^n \le b^n(1-s)^n$, which merges the two integrals into a single one multiplied by the factor $|E|b^n - D$; the sign of this factor then dictates whether the mixed term can be discarded (when $|E|b^n \le D$) or must be retained with the explicit majorant $t^{m+n+1}/(n+1)$ (when $|E|b^n > D$). The following theorem is the main technical estimate of this paper.

Theorem 1. *Let $m \in \mathbb{N}$, $n > 0$, $0 < b < 1$, and $ab^m \neq 1$. Then, for every $t \in (0,1)$,*

$$I(t) \le Q(b,n)t^{2m} + \frac{t^{2n+1}}{2n+1} + \max\left\{0, \frac{2(|E|b^n - D)}{n+1}\right\} t^{m+n+1}. \tag{18}$$

Consequently,

$$\sup_{0<t<1} I(t) \le Q(b,n) + \frac{1}{2n+1} + \max\left\{0, \frac{2(|E|b^n - D)}{n+1}\right\}. \tag{19}$$

https://doi.org/10.3390/math14152840

Equivalently,

$$\sup_{0<t<1}\int_0^1 \mathbf{Gr}^2(t,s)\,ds \le \frac{1}{\Gamma(\alpha)^2}\left[Q(b,n)+\frac{1}{2n+1}+\max\left\{0,\frac{2(|E|b^n-D)}{n+1}\right\}\right]. \tag{20}$$

Proof. According to relation (15) of Lemma 2, we have

$$I(t)=Q(b,n)t^{2m}+\frac{t^{2n+1}}{2n+1}+2[I_2(t)-I_1(t)].$$

For $0\le s\le \min(t,b)$, we have $b-s\le b(1-s)$, because this is equivalent to $s(1-b)\ge 0$. Since $n>0$, it follows that $(b-s)^n\le b^n(1-s)^n$. Thus,

$$\int_0^{\min(t,b)}(t-s)^n(b-s)^n\,ds \le b^n\int_0^t (t-s)^n(1-s)^n\,ds.$$

Therefore,

$$I_2(t)\le |E|\,b^n t^m\int_0^t (t-s)^n(1-s)^n\,ds. \tag{21}$$

Using (16), we obtain

$$I_2(t)-I_1(t)\le (|E|b^n-D)t^m\int_0^t (t-s)^n(1-s)^n\,ds. \tag{22}$$

Since $0\le s\le t<1$, we have $(1-s)^n\le 1$. Hence

$$\int_0^t (t-s)^n(1-s)^n\,ds \le \int_0^t (t-s)^n\,ds=\frac{t^{n+1}}{n+1}. \tag{23}$$

If $|E|b^n-D\le 0$, then (22) gives

$$I_2(t)-I_1(t)\le 0.$$

If $|E|b^n-D>0$, then (22) and (23) give

$$I_2(t)-I_1(t)\le \frac{|E|b^n-D}{n+1}t^{m+n+1}.$$

Combining the two cases yields

$$2(I_2(t)-I_1(t))\le \max\left\{0,\frac{2(|E|b^n-D)}{n+1}\right\}t^{m+n+1}.$$

Substituting this into (15) proves (18). Since $0<t<1$, all powers of t appearing in (18) are bounded above by 1, and hence (19) follows upon taking the supremum over $t\in(0,1)$; we write sup rather than max because $(0,1)$ is open (in fact I extends continuously to $[0,1]$, so the supremum coincides with the maximum of the extension over $[0,1]$). Finally, (20) follows from (14). □

In the regime $|E|b^n\le D$, the proof of Theorem 1 replaces the strictly negative mixed contribution $2[I_2(t)-I_1(t)]$ by zero. The following proposition retains this negative term and thereby produces a strictly sharper pointwise bound.

Proposition 1. *Assume $|E|b^n\le D$ (which forces $D>0$). Then, for every $t\in(0,1)$,*

$$I(t)\;\le\;\Phi(t)=Q(b,n)\,t^{2m}+\frac{t^{2n+1}}{2n+1}-2\big(D-|E|b^n\big)\,t^m P(t,n), \tag{24}$$

where, by Lemma 1 applied with b replaced by t,

$$P(t,n) = \int_0^t (1-s)^n (t-s)^n \, ds = \frac{t^{n+1}}{n+1} \, {}_2F_1(-n, 1; n+2; t).$$

If $D > |E|b^n$, the bound (24) is strictly smaller than the right-hand side of (18) for every $t \in (0,1)$.

Proof. By (16) and (9) we have the *exact* identity $I_1(t) = D\, t^m P(t,n)$. We bound I_2. Suppose first $E \geq 0$. For $0 \leq s \leq \min(t,b)$ we have $(b-s)^n \leq b^n (1-s)^n$, and since the integrand is nonnegative the domain of integration may be enlarged from $[0, \min(t,b)]$ to $[0,t]$; hence

$$I_2(t) \;\leq\; E\, b^n t^m \int_0^t (t-s)^n (1-s)^n \, ds = |E|\, b^n t^m P(t,n).$$

If $E < 0$, then $I_2(t) \leq 0 \leq |E|\, b^n t^m P(t,n)$. In both cases,

$$I_2(t) - I_1(t) \;\leq\; -\big(D - |E| b^n\big)\, t^m P(t,n),$$

and (24) follows from (15). Finally, when $D > |E|b^n$ the retained term $-2(D - |E|b^n) t^m P(t,n)$ is strictly negative on $(0,1)$ because $P(t,n) > 0$, whereas in (18) this contribution was discarded. □

Remark 2 (Interpretation of the regime $|E|b^n \leq D$)**.** *The hypothesis $|E|b^n \leq D$ of Proposition 1 admits a transparent reformulation in the original parameters:*

$$|E|b^n \leq D \quad \Longleftrightarrow \quad ab^{c-1} < 1 \;\; \text{and} \;\; |a| \leq b^{1-\alpha}.$$

Indeed, since $E = aD$ and $|E|b^n = |a|\,|D|\,b^n \geq 0$, the hypothesis forces $D > 0$, which is precisely $ab^m = ab^{c-1} < 1$; dividing $|a| D\, b^n \leq D$ by $D > 0$ then gives $|a| \leq b^{-n} = b^{1-\alpha}$. Conversely, if both conditions hold, then $D > 0$ and multiplying $|a|b^n \leq 1$ by D recovers the hypothesis. Note that for $\alpha < c$ the first condition is redundant, because $|a| \leq b^{1-\alpha}$ already implies $|a|b^m \leq b^{c-\alpha} < 1$; it does real work only in the limiting case $\alpha = c$, where it excludes the point $a = b^{1-c}$ at which $ab^m = 1$ and D is undefined. Geometrically, the admissible set of boundary multipliers is the interval $-b^{1-\alpha} \leq a \leq b^{1-\alpha}$ (with $a = b^{1-c}$ removed when $\alpha = c$). For $a > 0$ and $\alpha < c$ this interval is bounded away from the singular value b^{1-c}; for the benchmark family of Section 7.5 ($\alpha = 4.5$, $b = \frac{1}{2}$) it reads $0 < a \leq 2^{3.5} \approx 11.314$, well below the singular value $2^4 = 16$, and its right endpoint is marked by the dotted vertical line $\delta = 0$ in Figure 4. The full admissible region in the (b,a)-plane is displayed in Figure 1: the shaded set lies below the curve $a = b^{1-\alpha}$ (the locus $\delta = 0$), which in turn lies strictly below the singular curve $a = b^{1-c}$ for every $b \in (0,1)$, the two curves meeting only at $b = 1$; the vertical section at $b = \frac{1}{2}$ recovers exactly the interval and the two thresholds just described. When $\alpha = c$ and $0 < ab^m < 1$, one has, moreover, $\delta = D - |E|b^n = 1$ identically (see Remark 14).

Corollary 1 (Closed-form refined global bound)**.** *Assume $|E|b^n \leq D$ and set $\delta = D - |E|b^n \geq 0$. If $\delta > 0$, let*

$$\tau = \frac{2n+1}{2\,(m+2n+1)\,\delta},$$

and define

$$G(\delta) = \begin{cases} \dfrac{1-2\delta}{2n+1}, & \text{if } \delta = 0 \text{ or } \tau \geq 1, \\[2ex] \dfrac{m\,\tau^{(2n+1)/m}}{(m+2n+1)(2n+1)}, & \text{if } \tau < 1. \end{cases}$$

Then

$$\sup_{0<t<1} I(t) \leq Q(b,n) + G(\delta) \leq Q(b,n) + \frac{1}{2n+1}, \tag{25}$$

and the second inequality is strict whenever $\delta > 0$.

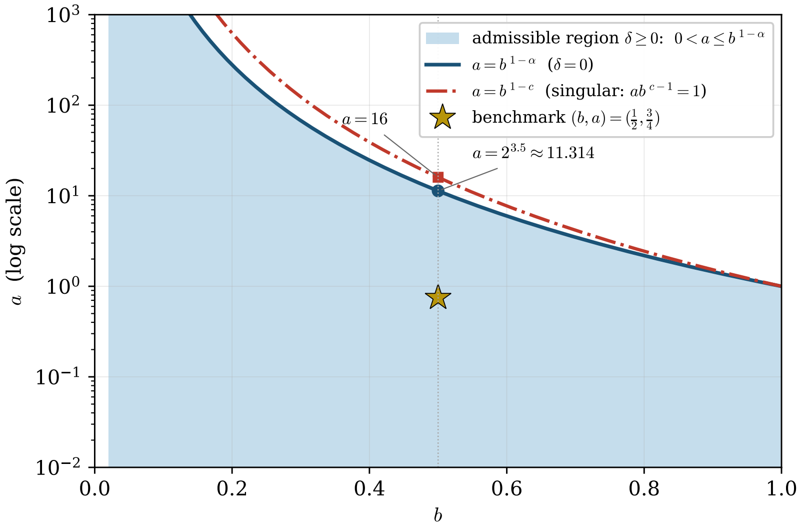

Figure 1. The admissible region $\{(b,a) : 0 < b < 1,\ 0 < a \leq b^{1-\alpha}\}$ of Proposition 1 and Corollary 1 (shaded), for $\alpha = 4.5$, $c = 5$, on a logarithmic vertical scale. The solid curve $a = b^{1-\alpha}$ is the locus $\delta = 0$; the dash-dotted curve $a = b^{1-c}$ is the singular set $ab^{c-1} = 1$, on which D and E diverge. For $\alpha < c$, the admissible boundary lies strictly below the singular curve for every $b \in (0,1)$, although the gap tends to zero as $b \to 1^-$. The star marks the benchmark configuration $(b,a) = (\frac{1}{2}, \frac{3}{4})$ of Section 7.4; the circle and square on the section $b = \frac{1}{2}$ mark the threshold $a = 2^{3.5} \approx 11.314$ and the singular value $a = 16$, i.e., the two vertical lines of Figure 4. By Remark 2 the region is symmetric under $a \mapsto -a$; only the half $a > 0$ relevant to the benchmark family is shown.

Proof. Since $1 - s \geq t - s \geq 0$ for $0 \leq s \leq t \leq 1$, we have $(1-s)^n \geq (t-s)^n$, whence

$$P(t,n) \geq \int_0^t (t-s)^{2n}\, ds = \frac{t^{2n+1}}{2n+1},$$

with equality if and only if $t = 1$. Since $\delta \geq 0$, substituting this lower bound into (24) gives

$$I(t) \leq Q(b,n)\, t^{2m} + g(t), \qquad g(t) = \frac{t^{2n+1} - 2\delta\, t^{m+2n+1}}{2n+1}.$$

Bounding $Q(b,n)t^{2m} \leq Q(b,n)$, it remains to maximise g on $[0,1]$. We compute

$$g'(t) = \frac{t^{2n}}{2n+1}\Big[(2n+1) - 2(m+2n+1)\,\delta\, t^m\Big],$$

so the only interior critical point satisfies $t_*^m = \tau$. If $\delta = 0$ or $\tau \geq 1$, then g is nondecreasing on $[0,1]$ and $\max g = g(1) = (1-2\delta)/(2n+1)$; note that $\tau \geq 1$ implies $2\delta \leq (2n+1)/(m+2n+1) < 1$, so this value is positive. If $\tau < 1$, the maximum is attained at $t_* = \tau^{1/m}$, and since $2\delta\tau = (2n+1)/(m+2n+1)$,

$$g(t_*) = \frac{\tau^{(2n+1)/m}}{2n+1}(1 - 2\delta\tau) = \frac{m\,\tau^{(2n+1)/m}}{(m+2n+1)(2n+1)}.$$

Finally, $G(\delta) < 1/(2n+1)$ for $\delta > 0$: in the first case this is immediate, and in the second it follows from $m\,\tau^{(2n+1)/m}/(m+2n+1) < 1$ since $0 < \tau < 1$. $\square$

Remark 3 (On the optimality of the closed-form bound)**.** *Corollary 1 is deliberately traded for explicitness rather than optimality. Exactly two inequalities are lossy in its proof: the kernel comparison* $P(t,n) \geq t^{2n+1}/(2n+1)$*, which is an equality only at* $t=1$*, and the decoupling* $Q(b,n)t^{2m} \leq Q(b,n)$*, which is an equality only at* $t=1$ *as well but is applied for all* t*. Consequently* $Q(b,n)+G(\delta)$ *is in general strictly larger than* $\sup_{0<t<1}\Phi(t)$*, and the residual gap can be substantial: for the benchmark parameters of Section 7.4 one has* $Q(b,n)+G(\delta) = 0.1308$ *while* $\sup_{0<t<1}\Phi(t) = 6.0402 \times 10^{-3}$*, so a direct numerical maximisation of* Φ *(Remark 6) improves the admissible constant by a further order of magnitude. The closed-form bound remains valuable because it requires no optimisation step and is monotone and elementary in the parameters.*

The magnitude of this loss is quantified in Section 7.4: the numerically maximised constant is $\Gamma(4.5)/\sqrt{\sup_{0<t<1}\Phi(t)} \approx 149.66$*, against the closed-form* $\mathcal{K}_B^* = 32.165$*. Its practical irrelevance for the solvability of the benchmark problem is illustrated by the convergence study of Section 7.6: the iteration converges for every value of* β *tested, the empirical convergence factor being far smaller than any a priori bound.*

4. Main Existence and Uniqueness Result

We now use the improved Green-function estimate to establish a Banach-type solvability condition.

Theorem 2. *Assume that* $h \in C([0,1]\times\mathbb{R},\mathbb{R})$ *satisfies the Lipschitz condition*

$$|h(t,x)-h(t,y)| \leq \mathcal{K}|x-y|, \qquad t\in[0,1], \quad x,y\in\mathbb{R}. \tag{26}$$

If

$$\mathcal{K} < \frac{\Gamma(\alpha)}{\sqrt{Q(b,n)+\dfrac{1}{2n+1}+\max\left\{0, \dfrac{2(|E|b^n-D)}{n+1}\right\}}}, \tag{27}$$

then problem (1) has a unique solution in $C([0,1])$*.*

Proof. We first record that every integral below is well defined and that the Cauchy–Schwarz step is legitimate. Since $h \in C([0,1]\times\mathbb{R},\mathbb{R})$ by (H1) and $u \in C([0,1])$, the composition $s \mapsto h(s,u(s))$ is continuous on the compact interval $[0,1]$, hence bounded, and therefore

$$h(\cdot,u(\cdot)) \in \mathbf{L}^\infty([0,1]) \subset \mathbf{L}^2([0,1]) \subset \mathbf{L}^1([0,1]).$$

By Remark 1 the map $\mathbf{Gr}(t,\cdot)$ is continuous on $[0,1]$ for each fixed $t\in[0,1]$, so $\mathbf{Gr}(t,\cdot) \in \mathbf{L}^2([0,1])$ as well. Consequently the product $\mathbf{Gr}(t,\cdot)\,h(\cdot,u(\cdot))$ is integrable, the operator T of (5) is well defined on $C([0,1])$, and the Cauchy–Schwarz inequality applied below to the pair $\big(|\mathbf{Gr}(t,\cdot)|,1\big) \in \mathbf{L}^2([0,1])\times\mathbf{L}^2([0,1])$ is justified.

For $u,v \in C([0,1])$, using (5) and (26), we obtain

$$|(Tu)(t)-(Tv)(t)| \leq \mathcal{K}\int_0^1 |\mathbf{Gr}(t,s)||u(s)-v(s)|\,ds.$$

Since $|u(s)-v(s)| \leq \|u-v\|_\infty$, it follows that

$$|(Tu)(t)-(Tv)(t)| \leq \mathcal{K}\|u-v\|_\infty \int_0^1 |\mathbf{Gr}(t,s)|\,ds.$$

By the Cauchy–Schwarz inequality,

$$\int_0^1 |\mathbf{Gr}(t,s)|\,ds \leq \left(\int_0^1 \mathbf{Gr}^2(t,s)\,ds\right)^{1/2}\left(\int_0^1 1\,ds\right)^{1/2} = \left(\int_0^1 \mathbf{Gr}^2(t,s)\,ds\right)^{1/2}.$$

Therefore,

$$|(Tu)(t) - (Tv)(t)| \leq \mathcal{K} \left(\int_0^1 \mathbf{Gr}^2(t,s)\, ds \right)^{1/2} \|u - v\|_\infty.$$

Taking the supremum over $t \in [0,1]$ and applying (20), we get

$$\|Tu - Tv\|_\infty \leq q\|u - v\|_\infty,$$

where

$$q = \frac{\mathcal{K}}{\Gamma(\alpha)} \sqrt{Q(b,n) + \frac{1}{2n+1} + \max\left\{0, \frac{2(|E|b^n - D)}{n+1}\right\}}.$$

Condition (27) implies $q < 1$. Hence T is a contraction on the complete metric space $C([0,1])$. By Banach's fixed-point theorem, T has a unique fixed point in $C([0,1])$. This fixed point is the unique solution of (1). □

Remark 4 (Why the improved estimate enlarges the admissible Lipschitz class)**.** *The mechanism behind the improvement is elementary but worth isolating. The contraction constant produced by the proof is $q = \mathcal{K}\,\Lambda^{1/2}/\Gamma(\alpha)$, where Λ denotes the global bound on $\sup_{0<t<1} \int_0^1 F^2(t,s)\, ds$; the admissible Lipschitz class is therefore $\mathcal{K} < \Gamma(\alpha)\Lambda^{-1/2}$, and* any *decrease of Λ enlarges it. The* $\mathbf{L}^1$ *analysis of [7] majorises the three terms of the Green function separately by their absolute values, which amounts to replacing the sign-definite mixed term $2[I_2(t) - I_1(t)]$ of (15) by its absolute value or worse; Theorem 1 replaces it by zero when $|E|b^n \leq D$, and Proposition 1 retains it in full. Each step strictly decreases Λ, hence strictly increases the admissible constant, which is exactly the ordering $\mathcal{K}_S \leq \mathcal{K}_B \leq \mathcal{K}_B^*$ observed in Sections 5 and 7.*

Remark 5 (Weaker Lipschitz-type assumptions)**.** *The global Lipschitz hypothesis (H2) can be relaxed along standard lines without altering the estimates of Section 3, which concern the Green function only. If h is merely locally Lipschitz, i.e., (26) holds for $x, y \in [-\rho, \rho]$ with constant $\mathcal{K}_\rho$, then the argument of Theorem 2 applies on the closed ball $B_\rho = \{u : \|u\|_\infty \leq \rho\}$ provided $T(B_\rho) \subseteq B_\rho$, which holds as soon as $\left(\mathcal{K}_\rho \rho + \sup_t |h(t,0)|\right)\sqrt{\Lambda}/\Gamma(\alpha) \leq \rho$ with Λ as in Remark 4; the conclusion is then uniqueness in B_ρ. Similarly, Lipschitz continuity can be replaced by a comparison function (φ-contraction) condition $|h(t,x) - h(t,y)| \leq \varphi(|x-y|)$ with φ nondecreasing and $\varphi(r)\sqrt{\Lambda}/\Gamma(\alpha) < r$ for $r > 0$, invoking the Boyd–Wong extension of Banach's principle. A systematic development is beyond the scope of this paper.*

In the regime $|E|b^n \leq D$, Corollary 1 yields the following sharper solvability condition.

Corollary 2. *Assume $|E|b^n \leq D$, set $\delta = D - |E|b^n \geq 0$, and let $G(\delta)$ be defined as in Corollary 1. Assume that $h \in C([0,1] \times \mathbb{R}, \mathbb{R})$ satisfies the Lipschitz condition (26). If*

$$\mathcal{K} \;<\; \mathcal{K}_B^* = \frac{\Gamma(\alpha)}{\sqrt{Q(b,n) + G(\delta)}}, \tag{28}$$

then problem (1) has a unique solution in $C([0,1])$. Moreover,

$$\mathcal{K}_B^* \;\geq\; \frac{\Gamma(\alpha)}{\sqrt{Q(b,n) + \dfrac{1}{2n+1} + \max\left\{0, \dfrac{2(|E|b^n - D)}{n+1}\right\}}},$$

with strict inequality whenever $\delta > 0$.

https://doi.org/10.3390/math14152840

Proof. The argument of Theorem 2 applies verbatim, with the estimate (19) replaced by (25); in view of (14), this amounts to replacing the bracket in (20) by $Q(b,n) + G(\delta)$, so that the contraction constant becomes

$$q = \frac{\mathcal{K}}{\Gamma(\alpha)} \sqrt{Q(b,n) + G(\delta)}\,,$$

and condition (28) implies $q < 1$. The comparison with the constant of Theorem 2 follows from the second inequality in (25), noting that $\max\{0, 2(|E|b^n - D)/(n+1)\} = 0$ in the regime $|E|b^n \le D$. □

Remark 6. *Even Corollary 2 is not optimal in the regime $|E|b^n < D$: the pointwise bound $\Phi(t)$ in (24) is an explicit elementary function of t, and $\sup\{\Phi(t),\ 0 < t < 1\}$ can be evaluated numerically to arbitrary accuracy, producing a still sharper admissible constant. Corollary 2 is stated as the main refinement because it provides a fully explicit, closed-form criterion in the parameters α, a, b, and c. None of the bounds of this paper is claimed to be sharp in the sense of being attained: the strict hierarchy $I(t) \le \Phi(t) \le Q(b,n)t^{2m} + t^{2n+1}/(2n+1)$ on $(0,1)$, established in Proposition 1 and verified numerically in Figure 2, shows that each successive bound leaves a positive gap, and Section 7.4 quantifies these gaps on the benchmark problem. The natural limit of the present method is the quantity $\sup_{0<t<1} \int_0^1 \mathbf{Gr}^2(t,s)\,ds$ itself, whose exact evaluation in closed form for arbitrary (α, a, b, c) appears to be out of reach and is left as an open problem; even this quantity would only be optimal within the $\mathbf{L}^2$/Cauchy–Schwarz strategy, not for the boundary value problem per se.*

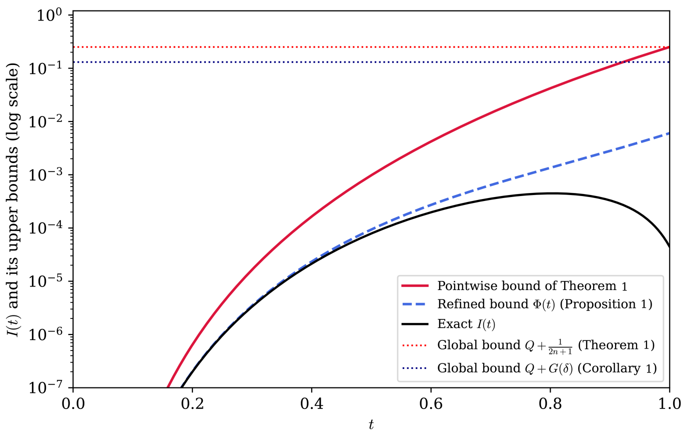

Figure 2. Benchmark example (44): exact $I(t)$ (solid black), pointwise bound of Theorem 1 (solid red), refined pointwise bound $\Phi(t)$ of Proposition 1 (dashed blue), and the global bounds of Theorem 1 and Corollary 1 (dotted horizontal lines), on a logarithmic vertical scale.

5. Comparison with Shivanian's Criterion

Shivanian's admissible Lipschitz constant is

$$\mathcal{K}_S = \frac{\Gamma(\alpha+1)}{2(1+|E|)}. \tag{29}$$

The admissible Lipschitz constant obtained from Theorem 2 is

$$\mathcal{K}_B = \frac{\Gamma(\alpha)}{\sqrt{Q(b,n) + \dfrac{1}{2n+1} + \max\left\{0, \dfrac{2(|E|b^n - D)}{n+1}\right\}}}. \tag{30}$$

Theorem 3. *The proposed Banach-type criterion is less restrictive than Shivanian's criterion, that is,*

$$\mathcal{K}_S \leq \mathcal{K}_B, \tag{31}$$

if and only if

$$Q(b,n) + \frac{1}{2n+1} + \max\left\{0, \frac{2(|E|b^n - D)}{n+1}\right\} \leq \frac{4(1+|E|)^2}{(n+1)^2}. \tag{32}$$

Proof. Since $n = \alpha - 1$, we have

$$\Gamma(\alpha+1) = \alpha\Gamma(\alpha) = (n+1)\Gamma(\alpha).$$

Therefore, by (29),

$$\mathcal{K}_S = \frac{(n+1)\Gamma(\alpha)}{2(1+|E|)}.$$

The inequality $\mathcal{K}_S \leq \mathcal{K}_B$ is equivalent to

$$\frac{(n+1)\Gamma(\alpha)}{2(1+|E|)} \leq \frac{\Gamma(\alpha)}{\sqrt{Q(b,n) + \frac{1}{2n+1} + \max\left\{0, \frac{2(|E|b^n - D)}{n+1}\right\}}}.$$

Since $\Gamma(\alpha) > 0$, canceling $\Gamma(\alpha)$ and squaring both positive sides gives exactly (32). Hence the result follows. □

Remark 7. *Condition* (32) *is not assumed to hold for all parameter values. Rather, it identifies the parameter regimes in which the new Banach-type criterion guarantees existence and uniqueness for a larger class of nonlinearities than Shivanian's condition.*

Remark 8 (Quantitative comparison of the contraction constants)**.** *The comparison of Theorem 3 can be phrased directly at the level of the contraction constants. For a fixed nonlinearity with Lipschitz constant $\mathcal{K}$, the $\mathbf{L}^1$-based argument of [7] yields the contraction constant $q_S = \mathcal{K}/\mathcal{K}_S$, while Theorem 2 yields $q = \mathcal{K}/\mathcal{K}_B$; hence*

$$\frac{q_S}{q} = \frac{\mathcal{K}_B}{\mathcal{K}_S} = R,$$

so the improvement factor R of (64) *measures precisely how much smaller the new contraction constant is, uniformly in $\mathcal{K}$. On the benchmark problem of Section 7.4, $R = 1.585$: the contraction constant is reduced by 37%, and by a factor $R^* = 2.196$ under Corollary 2. Table 5 reports R and R^* across six parameter configurations.*

Table 2 juxtaposes, feature by feature, the criterion of [7] and the criteria obtained in this paper.

Table 2. Summary of the solvability criteria for problem (1) and of the results available under each. "CD" abbreviates continuous dependence on data.

	Shivanian [7]	**Theorem 2**	**Corollary 2**
Kernel estimate	uniform $\mathbf{L}^1$	$\mathbf{L}^2$ (Theorem 1)	$\mathbf{L}^2$ refined (Corollary 1)
Admissible constant	$\mathcal{K}_S$ in (29)	$\mathcal{K}_B$ in (30)	$\mathcal{K}_B^*$ in (28)
Validity	all admissible parameters	all admissible parameters	$\delta = D - \lvert E\rvert b^n \geq 0$
Benchmark value	14.646	23.220	32.165
Ulam–Hyers stability	not explicitly established in [7]; follows from the same contraction argument whenever $q_S < 1$	Theorem 4	Remark 9
CD in h and a	not explicitly established in [7]; likewise obtainable from the same contraction argument whenever $q_S < 1$	Theorem 5, Proposition 2	(same, with q^*)

6. Ulam–Hyers Stability

We establish that the solution guaranteed by Theorem 2 is Ulam–Hyers stable. Recall the standard notion: a solution u^* of (1) is *Ulam–Hyers (UH) stable* if there exists a constant $C_{\mathrm{UH}} > 0$ such that, for every $\varepsilon > 0$ and every $\tilde{u} \in C([0,1])$ satisfying

$$\left\| \tilde{u} - \int_0^1 \mathbf{Gr}(\cdot, s)\, h(s, \tilde{u}(s))\, ds \right\|_\infty \le \varepsilon, \tag{33}$$

one has $\|\tilde{u} - u^*\|_\infty \le C_{\mathrm{UH}}\, \varepsilon$.

We adopt this operator-level formulation because it is meaningful for every $\tilde{u} \in C([0,1])$. Its relation to the differential formulation is as follows. Assume that

(i) $D_t^\alpha \tilde{u}$ exists on $(0,1)$ and the Green representation of Section 2 applies to $\tilde{u}$ (it suffices, for instance, that $\tilde{u} \in C^c([0,1])$ with $D_t^\alpha \tilde{u} \in C((0,1)) \cap \mathbf{L}^1(0,1)$);

(ii) $\tilde{u}$ satisfies the boundary conditions of (1) *exactly*, that is $\tilde{u}(0) = \tilde{u}'(0) = \cdots = \tilde{u}^{(c-2)}(0) = 0$ and $\tilde{u}(1) = a\, \tilde{u}(b)$; and

(iii) The differential residual $r(t) = D_t^\alpha \tilde{u}(t) + h(t, \tilde{u}(t))$ satisfies $|r(t)| \le \varepsilon$ on $(0,1)$.

Rewriting (iii) as $D_t^\alpha \tilde{u}(t) + \big[h(t, \tilde{u}(t)) - r(t)\big] = 0$ and invoking (ii), the function $\tilde{u}$ solves (1) with the nonlinearity $h(\cdot, \tilde{u}(\cdot)) - r(\cdot)$ and with exactly the boundary data inverted by the Green operator. The representation of Section 2 therefore gives

$$\tilde{u}(t) = \int_0^1 \mathbf{Gr}(t,s)\big[h(s, \tilde{u}(s)) - r(s)\big]\, ds,$$

whence

$$\tilde{u}(t) - \int_0^1 \mathbf{Gr}(t,s)\, h(s, \tilde{u}(s))\, ds = -\int_0^1 \mathbf{Gr}(t,s)\, r(s)\, ds.$$

By the Cauchy–Schwarz inequality and the bound (20),

$$\left| \int_0^1 \mathbf{Gr}(t,s)\, r(s)\, ds \right| \le \varepsilon \left(\int_0^1 \mathbf{Gr}^2(t,s)\, ds \right)^{1/2} \le \frac{\varepsilon\sqrt{\Lambda}}{\Gamma(\alpha)}$$

uniformly in $t \in [0,1]$, where Λ denotes the global bound of Remark 4. Hence (33) holds with ε replaced by $\varepsilon\sqrt{\Lambda}/\Gamma(\alpha)$: every function obeying the differential residual bound obeys the operator residual bound, and the differential formulation is a special case of the operator formulation, with stability constant $C_{\mathrm{UH}}^B \sqrt{\Lambda}/\Gamma(\alpha)$. We stress that (ii) is used in an essential way; if $\tilde{u}$ satisfies the boundary conditions only approximately, an additional term quantifying the boundary defect must be carried through the representation, which we do not pursue here.

Theorem 4 (Ulam–Hyers stability)**.** *Under the hypotheses of Theorem 2, let $q < 1$ denote the contraction constant*

$$q = \frac{\mathcal{K}}{\Gamma(\alpha)} \sqrt{Q(b,n) + \frac{1}{2n+1} + \max\left\{0, \frac{2(|E| b^n - D)}{n+1}\right\}}. \tag{34}$$

Then the unique solution $u^* \in C([0,1])$ of (1) is Ulam–Hyers stable with stability constant

$$C_{\mathrm{UH}}^B = \frac{1}{1-q}. \tag{35}$$

Proof. Let $\varepsilon > 0$ and let $\tilde{u} \in C([0,1])$ satisfy (33). Define the integral operator T by $(Tu)(t) = \int_0^1 \mathbf{Gr}(t,s) h(s, u(s))\, ds$. Since $u^* = Tu^*$, we have

$$\begin{aligned} \|\tilde{u} - u^*\|_\infty &\le \|\tilde{u} - T\tilde{u}\|_\infty + \|T\tilde{u} - Tu^*\|_\infty \\ &\le \varepsilon + q\, \|\tilde{u} - u^*\|_\infty, \end{aligned}$$

where the second term uses the Lipschitz condition (26), the Cauchy–Schwarz inequality, and the bound (20), exactly as in the proof of Theorem 2. Rearranging gives $\|\tilde{u} - u^*\|_\infty \leq \varepsilon/(1-q)$, which is the UH stability condition with $C^B_{\mathrm{UH}} = (1-q)^{-1}$. □

Remark 9. *The stability constant $C^B_{\mathrm{UH}} = (1-q)^{-1}$ is a strictly increasing function of q on $[0,1)$, since $\frac{d}{dq}(1-q)^{-1} = (1-q)^{-2} > 0$. Since the refined $\mathbf{L}^2$ estimate produces a smaller q than the $\mathbf{L}^1$-based estimate of [7], the present result simultaneously extends the range of $\mathcal{K}$ for which UH stability is guaranteed and yields a smaller (i.e., tighter) stability constant. Under the hypotheses of Corollary 2, the further improved constant $q^* = (\mathcal{K}/\Gamma(\alpha))\sqrt{Q(b,n) + G(\delta)}$ satisfies $q^* \leq q$, so the stability constant $C^*_{\mathrm{UH}} = (1-q^*)^{-1}$ is at most as large as C^B_{UH}. We do not claim that $(1-q)^{-1}$ is the* optimal *(smallest possible) stability constant for problem (1): it is the canonical constant delivered by the contraction argument, and it is optimal only within that argument, in the sense that it decreases monotonically with every improvement of the bound on $\sup_{0<t<1}\int_0^1 \mathbf{Gr}^2(t,s)\,ds$. Determining the minimal Ulam–Hyers constant is an open question even for much simpler classes of fractional boundary value problems.*

Remark 10 (Relation to iterative linearisation schemes)**.** *We note a methodological kinship with iterative linearisation schemes such as the L-scheme for degenerate nonlinear diffusion problems [37], whose convergence likewise rests on a tightly bounded contraction factor produced by a stabilising term. The objects controlled are however different—the L-scheme concerns the a posteriori convergence of an iterative solver, whereas Ulam–Hyers stability is an a priori property of the exact fixed point—so the respective constants are not directly comparable. The principle common to both, and the one exploited throughout this paper, is that any sharpening of the governing contraction constant immediately tightens the resulting guarantee.*

Example 1. *For the benchmark problem (44) with $\beta = 40$, the sharp Lipschitz constant (46) is $L = 20$, which lies beyond Shivanian's threshold $\mathcal{K}_S = 14.646$ but below $\mathcal{K}_B$; Theorem 2 gives $q = L/\mathcal{K}_B = 20/23.220 \approx 0.8613$, hence $C^B_{\mathrm{UH}} \approx 7.21$. For $\beta = 60$ one has $L = 30$, beyond both $\mathcal{K}_S$ and $\mathcal{K}_B$; Corollary 2 gives $q^* = L/\mathcal{K}^*_B = 30/32.165 \approx 0.9327$, hence $C^*_{\mathrm{UH}} \approx 14.85$.*

7. Numerical Results and Continuous Dependence on Data

This section collects all numerical illustrations of the paper and the associated continuous-dependence theory. Sections 7.1 and 7.2 establish explicit sensitivity bounds on the solution with respect to perturbations of the nonlinearity h and the boundary parameter a, respectively. Section 7.3 illustrates these bounds numerically. Section 7.4 examines the Green-function bounds and admissible Lipschitz constants on the benchmark problem, and Section 7.5 compares the three solvability criteria across a broad range of parameter configurations.

Reproducibility. All computations reported in this section were carried out in Python 3.12.3 with NumPy 2.4.4 and `mpmath` 1.3.0. High-precision evaluations used a working precision of `mp.dps` = 40 decimal digits. The definite integrals—$I(t)$ in (13), $Q(b,n)$ in (10), and the kernel $\mathbf{L}^1$ and $\mathbf{L}^2$ norms — were evaluated by composite Simpson quadrature on a uniform grid of 1201 nodes and independently cross-checked against the adaptive routine `mpmath.quad`; the closed forms of Lemma 1 agree with direct quadrature of the definitions to machine precision. The suprema over t (of I, Φ and the kernel norms) were approximated by taking the maximum over the same uniform grid. Grid refinement from $N = 301$ to $N = 4801$ changes the estimated kernel norm from 1.4113457×10^{-3} to 1.4113224×10^{-3}, an absolute difference of 2.33×10^{-8}. The values therefore agree to approximately five significant digits, and we report the norm as 1.4113×10^{-3}. The Gauss hypergeometric value ${}_2F_1(-n,1;n+2;b)$ was evaluated with `mpmath.hyp2f1`. The one-dimensional maximisation of Φ (Remark 6) used bounded golden-section search on $[0,1]$

with tolerance 10^{-12}. Figures 1–4 use 1000 uniformly spaced sample points. The fixed-point iteration of Section 7.6 uses the same 1201-node Simpson rule with the discrete Green matrix assembled once, starting value $u_0 \equiv 0$, and stopping criterion $\|u_k - u_{k-1}\|_\infty < 10^{-6}$; the reported times are the median of 100 repeated solves, measured in double precision on an ×86-64 Linux machine, and exclude the one-off construction of the Green matrix. The complete Python script that generates every constant, table and figure of this section is provided in the Supplementary Materials.

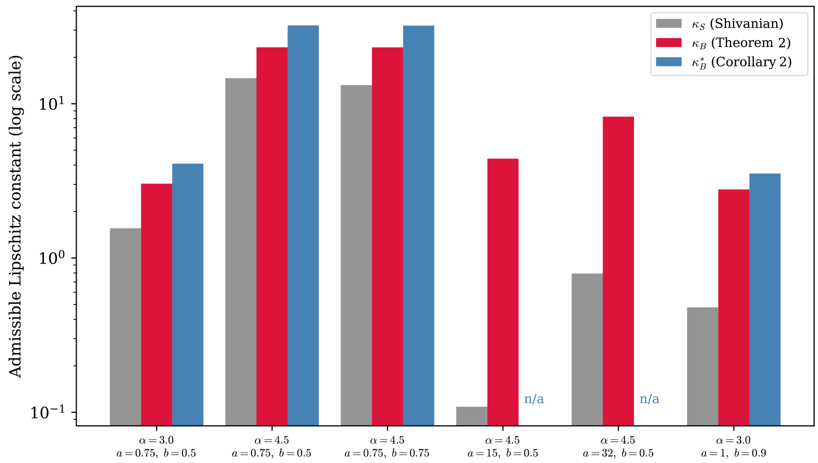

Figure 3. Admissible Lipschitz constants $\mathcal{K}_S$ (Shivanian), $\mathcal{K}_B$ (Theorem 2), and $\mathcal{K}_B^*$ (Corollary 2) for the six parameter configurations of Table 5, on a logarithmic scale. The label "n/a" indicates configurations with $\delta < 0$, for which Corollary 2 does not apply.

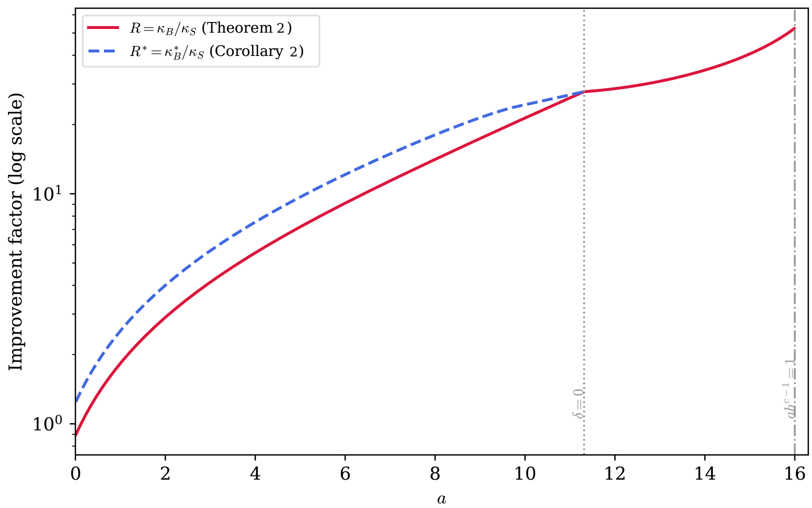

Figure 4. Improvement factors $R = \mathcal{K}_B/\mathcal{K}_S$ and $R^* = \mathcal{K}_B^*/\mathcal{K}_S$ as functions of a, for $\alpha = 4.5$, $c = 5$, $b = \frac{1}{2}$, on a logarithmic vertical scale. The dotted vertical line marks $\delta = 0$ (i.e., $a = 2^{3.5}$), beyond which Corollary 2 no longer applies; the dash-dotted vertical line marks the singular regime $ab^{c-1} = 1$ (i.e., $a = 16$).

7.1. Dependence on the Nonlinearity

Theorem 5 (Continuous dependence on h)**.** *Suppose $h_1, h_2 \in C([0,1] \times \mathbb{R}, \mathbb{R})$ both satisfy the Lipschitz condition (26) with the same constant $\mathcal{K}$ satisfying (27), and let $u_1^*, u_2^* \in C([0,1])$ be the corresponding unique solutions of (1). Define*

$$\sigma = \sup_{t \in [0,1]} |h_1(t, u_1^*(t)) - h_2(t, u_1^*(t))|. \tag{36}$$

Then

$$\|u_1^* - u_2^*\|_\infty \ \le \ \frac{\sigma}{(1-q)\,\Gamma(\alpha)}\sqrt{Q(b,n) + \frac{1}{2n+1} + \max\Big\{0, \frac{2(|E|b^n - D)}{n+1}\Big\}}, \tag{37}$$

where $q < 1$ is the contraction constant (34).

Proof. Let T_i denote the integral operator associated with h_i, so that $u_i^* = T_i u_i^*$. Write

$$\|u_1^* - u_2^*\|_\infty \le \|T_1 u_1^* - T_2 u_1^*\|_\infty + \|T_2 u_1^* - T_2 u_2^*\|_\infty.$$

The second term satisfies $\|T_2 u_1^* - T_2 u_2^*\|_\infty \le q\|u_1^* - u_2^*\|_\infty$, because h_2 satisfies (26) with the same constant $\mathcal{K}$ and hence T_2 is a contraction with the same constant q, by the argument of Theorem 2. The first term is evaluated at u_1^*, in accordance with the definition (36) of σ: using the Cauchy–Schwarz inequality and (20),

$$\begin{aligned}|(T_1u_1^*)(t) - (T_2u_1^*)(t)| &= \left|\int_0^1 \mathbf{Gr}(t,s)\,[h_1(s,u_1^*(s)) - h_2(s,u_1^*(s))]\,ds\right| \\ &\le \sigma\int_0^1 |\mathbf{Gr}(t,s)|\,ds \ \le \ \frac{\sigma}{\Gamma(\alpha)}\sqrt{Q(b,n) + \frac{1}{2n+1} + \max\Big\{0, \frac{2(|E|b^n - D)}{n+1}\Big\}},\end{aligned}$$

uniformly in $t \in [0,1]$. Combining the two estimates,

$$\|u_1^* - u_2^*\|_\infty \le \frac{\sigma}{\Gamma(\alpha)}\sqrt{Q(b,n) + \frac{1}{2n+1} + \max\Big\{0, \frac{2(|E|b^n - D)}{n+1}\Big\}} + q\,\|u_1^* - u_2^*\|_\infty,$$

and since $q < 1$, transposing the last term and dividing by $(1-q) > 0$ gives (37). □

Remark 11. *The bound* (37) *is explicit and computable from the problem parameters. Since the denominator $(1-q)$ is larger under the refined $\mathbf{L}^2$ estimate than it would be under the coarser $\mathbf{L}^1$ estimate of [7] (because the refined estimate yields a smaller q), the new framework provides a* tighter *sensitivity bound: the solution is certified to change by less than the $\mathbf{L}^1$-based analysis predicts. We also note that the bound* (37)*, like every result of this paper, is valid for* all *admissible orders $\alpha \in (c-1, c]$ with $c \in \mathbb{N}$, $c \ge 2$: the proofs use only $n = \alpha - 1 > 0$ together with (H0), and no additional restriction on α is introduced at any point. The same applies to Proposition 2 below.*

7.2. Dependence on the Boundary Parameter

The boundary condition $u(1) = a\,u(b)$ enters through the constants D and E defined in (6). Perturbing a to $\tilde{a}$ (with $\tilde{a}b^m \ne 1$) produces perturbed constants $\tilde{D}, \tilde{E}$ and a perturbed Green function $\tilde{\mathbf{Gr}}(t,s) = \mathbf{Gr}(t,s;\tilde{a})$. Let u^* and $\tilde{u}^*$ be the respective solutions.

Proposition 2 (Continuous dependence on a)**.** *Assume the Lipschitz condition* (26) *holds and both $\mathcal{K}_B(a)$ and $\mathcal{K}_B(\tilde{a})$ exceed $\mathcal{K}$, so that both u^* and $\tilde{u}^*$ exist and are unique. Then*

$$\|u^* - \tilde{u}^*\|_\infty \ \le \ \frac{1}{1-\tilde{q}}\sup_{t\in[0,1]}\left(\int_0^1 |\mathbf{Gr}(t,s;\tilde{a}) - \mathbf{Gr}(t,s;a)|\,|h(s,u^*(s))|\,ds\right), \tag{38}$$

where $\tilde{q} < 1$ is the contraction constant of $\tilde{T}$ computed with $\tilde{a}$. In particular, $\|u^* - \tilde{u}^*\|_\infty \to 0$ as $\tilde{a} \to a$.

Proof. Since $u^* = Tu^*$ and $\tilde{u}^* = \tilde{T}\tilde{u}^*$, write

$$\|u^* - \tilde{u}^*\|_\infty \le \|\tilde{T}u^* - \tilde{T}\tilde{u}^*\|_\infty + \|Tu^* - \tilde{T}u^*\|_\infty \le \tilde{q}\|u^* - \tilde{u}^*\|_\infty + \|Tu^* - \tilde{T}u^*\|_\infty.$$

For the last term, the pointwise identity $(Tu^*)(t) - (\tilde{T}u^*)(t) = \int_0^1 \big[\mathbf{Gr}(t,s;a) - \mathbf{Gr}(t,s;\tilde{a})\big]$
$h(s,u^*(s))\,ds$ gives

$$\big\|Tu^* - \tilde{T}u^*\big\|_\infty \le \sup_{t\in[0,1]} \int_0^1 |\mathbf{Gr}(t,s;\tilde{a}) - \mathbf{Gr}(t,s;a)|\,|h(s,u^*(s))|\,ds;$$

transposing $\tilde{q}\|u^* - \tilde{u}^*\|_\infty$ and dividing by $(1-\tilde{q}) > 0$ gives (38). Continuity in a follows because $\mathbf{Gr}(t,s;a)$ is continuous in a uniformly in (t,s) whenever $ab^m \neq 1$, so the supremum in (38) tends to zero as $\tilde{a} \to a$. $\square$

Remark 12. *The bound* (38) *characterizes dependence on the boundary multiplier only while both the original and perturbed operators remain contractions. For a fixed Lipschitz constant $\mathcal{K} > 0$, the contraction-valid interval ends at the first parameter value for which $\mathcal{K}_B(\tilde{a}) = \mathcal{K}$. As this threshold is approached from below, $\tilde{q} = \mathcal{K}/\mathcal{K}_B(\tilde{a}) \uparrow 1$ and the factor $(1-\tilde{q})^{-1}$ diverges. Separately, the coefficients D and E, and hence the Green kernel itself, diverge as $a \to (b^{1-c})^-$. This explains the deterioration near resonance, but it does not extend the validity of* (38) *beyond the point at which $\tilde{q} \ge 1$.*

Remark 13 (Dependence on the remaining model parameters)**.** *The argument of Proposition 2 is not specific to the multiplier a and extends verbatim to the other data of the problem. (i) Perturbing the interior node b to $\tilde{b}$ (with $a\tilde{b}^m \neq 1$) changes the Green function through D, E and the truncated power $(b-s)_+^n$; since $\mathbf{Gr}(t,s;b)$ is continuous in b uniformly in (t,s) away from the singular set $ab^m = 1$, the same two-term splitting yields $\|u^* - \tilde{u}^*\|_\infty \le (1-\tilde{q})^{-1}\sup_t \int_0^1 |\mathbf{Gr}(t,s;\tilde{b}) - \mathbf{Gr}(t,s;b)|\,|h(s,u^*(s))|\,ds \to 0$ as $\tilde{b} \to b$. (ii) Perturbing the order α affects* $\mathbf{Gr}$ *through $\Gamma(\alpha)$ and the exponents $n = \alpha - 1$; for $\alpha, \tilde{\alpha}$ in a compact subset of $(c-1,c]$ the kernel is uniformly continuous in α, and the identical estimate applies. We confine the detailed quantitative bounds (analogues of* (42)*) to the case of a, which is the parameter of greatest structural interest here because of the singular regime $ab^{c-1} = 1$.*

7.3. Numerical Illustration of the Continuous-Dependence Bounds

We illustrate the bounds of Theorem 5 and Proposition 2 on the benchmark problem (44) with parameters (48), both displayed in Section 7.4 below. Recall $\mathcal{K}_B = 23.220$, $\Lambda_B = Q(b,n) + \frac{1}{2n+1} = 0.2509$, and $\Gamma(4.5) = 11.6317$.

7.3.1. Sensitivity with Respect to the Nonlinearity

Consider the perturbed problem obtained by replacing h in (44) by

$$h_2(t,w) = \beta\frac{w}{1+\cosh(w)} + \cos\left(\frac{t}{4}\right) + \varepsilon\sin(\pi t), \tag{39}$$

where $\varepsilon > 0$ is a small perturbation amplitude. Both h and h_2 have the sharp Lipschitz constant $L = \beta/2$ in w, by (46). Since $|h(t,u) - h_2(t,u)| = \varepsilon|\sin(\pi t)| \le \varepsilon$, we have $\sigma = \varepsilon$ in Theorem 5, and the sensitivity bound (37) reads

$$\|u_1^* - u_2^*\|_\infty \;\le\; C_h^B\,\varepsilon, \qquad C_h^B = \frac{\sqrt{\Lambda_B}}{\Gamma(\alpha)(1-q)}, \quad q = \frac{L}{\mathcal{K}_B} = \frac{\beta}{2\mathcal{K}_B}. \tag{40}$$

For comparison, Shivanian's $\mathbf{L}^1$-based analysis (valid only for $L < \mathcal{K}_S$, i.e., $\beta < 29.293$) gives the analogous bound with constant

$$C_h^S = \frac{1}{\mathcal{K}_S(1-q_S)}, \qquad q_S = \frac{L}{\mathcal{K}_S} = \frac{\beta}{2\mathcal{K}_S}. \tag{41}$$

Table 3 reports q, C_h^B, q_S and C_h^S for $\beta \in \{10, 20, 30, 40\}$, that is, for sharp Lipschitz constants $L \in \{5, 10, 15, 20\}$. For $\beta \geq 30$ (that is $L \geq 15$) the $\mathbf{L}^1$-based bound is inapplicable, since then $L > \mathcal{K}_S$; for $\beta < 30$ the ratio C_h^S / C_h^B shows that the $\mathbf{L}^2$-based bound is strictly tighter, the improvement growing from a factor of 1.89 at $\beta = 10$ to a factor of 2.85 at $\beta = 20$.

Table 3. Sensitivity constants for a perturbation $\varepsilon \sin(\pi t)$ added to h, for the benchmark parameters (48). The column C_h^S / C_h^B gives the tightening factor of the $\mathbf{L}^2$ bound over the $\mathbf{L}^1$ bound; "n/a" indicates that the $\mathbf{L}^1$-based criterion is inapplicable since then $L \geq \mathcal{K}_S = 14.646$. The criteria are applied to the sharp Lipschitz constant $L = \beta/2$ of (46).

β	$L = \beta/2$	$q = L/\mathcal{K}_B$	$1 - q$	C_h^B	$q_S = L/\mathcal{K}_S$	C_h^S	C_h^S/C_h^B
10	5	0.2153	0.7847	0.0549	0.3414	0.1037	1.89
20	10	0.4307	0.5693	0.0756	0.6828	0.2152	2.85
30	15	0.6460	0.3540	0.1217	n/a	n/a	n/a
40	20	0.8613	0.1387	0.3106	n/a	n/a	n/a

7.3.2. Sensitivity with Respect to the Boundary Parameter

We fix $\beta = 20$, that is, the sharp Lipschitz constant $L = \beta/2 = 10$, and perturb the boundary parameter $a = 0.75$ to $\tilde{a} = a + \Delta a$. To bound the right-hand side of (38), we use the $\mathbf{L}^1$ estimate

$$\sup_{t \in [0,1]} \int_0^1 |\mathbf{Gr}(t, s; \tilde{a}) - \mathbf{Gr}(t, s; a)|\, ds \;\leq\; \frac{|\Delta D| \,+\, |\Delta E|\, b^{n+1}}{\Gamma(\alpha)(n+1)}, \tag{42}$$

where $\Delta D = \tilde{D} - D$ and $\Delta E = \tilde{E} - E$. It remains to control the nonlinear factor $M = \sup_{s \in [0,1]} |h(s, u^*(s))|$. Splitting $u^* = Tu^* = (Tu^* - T0) + T0$, where 0 denotes the zero function, and using the contraction estimate $\|Tu^* - T0\|_\infty \leq q\|u^*\|_\infty$ together with $\|T0\|_\infty \leq \sqrt{\Lambda_B}/\Gamma(\alpha)$ (by the Cauchy–Schwarz argument of Theorem 2 and $|h(s, 0)| = |\cos(s/4)| \leq 1$), we obtain $\|u^*\|_\infty \leq \sqrt{\Lambda_B}/\big(\Gamma(\alpha)(1 - q)\big) = 0.0756$ for $L = 10$; hence, by the Lipschitz condition, $M \leq 1 + L\|u^*\|_\infty \leq 1.76$. Combining this with (42) in (38) gives the fully explicit sensitivity bound

$$\|u^* - \tilde{u}^*\|_\infty \;\leq\; M\, \frac{|\Delta D| + |\Delta E|\, b^{n+1}}{\Gamma(\alpha)(n+1)(1 - \tilde{q})}, \tag{43}$$

where $\tilde{q} = L/\mathcal{K}_B(\tilde{a}) = \beta/\big(2\mathcal{K}_B(\tilde{a})\big)$ and $M \leq 1.76$. Before presenting the numbers, we clarify the two distinct thresholds in a that appear in this paper for the family $\alpha = 4.5$, $c = 5$, $b = \frac{1}{2}$: the threshold $\delta = 0$, attained at $a = 2^{3.5} \approx 11.314$, beyond which the refined criterion of Corollary 2 ceases to apply (cf. Remark 2), and the singular value $ab^{c-1} = 1$, attained at $a = 16$, at which D and E diverge and the boundary condition degenerates. All perturbations considered in Table 4 keep $\tilde{a} \leq 1.25$, far below both thresholds. Table 4 displays the kernel factor $\big(|\Delta D| + |\Delta E|\, b^{n+1}\big)/\big(\Gamma(\alpha)(n+1)(1 - \tilde{q})\big)$, i.e., the bound (43) normalised by M, for $\Delta a \in \{0.01, 0.05, 0.10, 0.20, 0.50\}$. The bound is small and nearly proportional to Δa for modest perturbations, confirming the expected first-order behaviour.

We emphasise the domain of validity of these estimates. Proposition 2 and the bounds (38) and (43) presuppose that *both* the original and the perturbed operators are contractions, that is $q = \mathcal{K}/\mathcal{K}_B(a) < 1$ and $\tilde{q} = \mathcal{K}/\mathcal{K}_B(\tilde{a}) < 1$; only then are u^* and $\tilde{u}^*$ guaranteed to exist, to be unique, and to satisfy the displayed inequalities. For a fixed Lipschitz constant, the contraction-valid interval ends at the first value a_{crit} for which $\mathcal{K}_B(a_{\mathrm{crit}}) = \mathcal{K}$. As $\tilde{a} \uparrow a_{\mathrm{crit}}$ from below, one has $\tilde{q} \uparrow 1$ and the factor $(1 - \tilde{q})^{-1}$ in (43) diverges. Once $\tilde{q} \geq 1$, the contraction hypothesis fails, Proposition 2 no longer applies, and (43) yields no conclusion. The Green kernel may continue to deteriorate as the singular value b^{1-c} is approached, but the contraction-based sensitivity estimate cannot be continued through the region where $\tilde{q} \geq 1$. All perturbations reported in Table 4 satisfy $\tilde{q} \leq 0.4313$ and lie comfortably within the range of validity.

Table 4. Sensitivity bound (43), normalised by the factor $M \leq 1.76$, for a perturbation Δa in the boundary parameter $a = 0.75$, with $\beta = 20$ (sharp Lipschitz constant $L = 10$) and benchmark parameters (48). All perturbed values $\tilde{a} = a + \Delta a \leq 1.25$ remain far below both the threshold $\delta = 0$ ($a = 2^{3.5} \approx 11.314$) and the singular value $a = 16$.

Δa	$\tilde{a} = a + \Delta a$	$\mathcal{K}_B(\tilde{a})$	$\tilde{q} = L/\mathcal{K}_B(\tilde{a})$	Sensitivity Bound
0.01	0.76	23.219	0.4307	3.9×10^{-5}
0.05	0.80	23.216	0.4307	2.0×10^{-4}
0.10	0.85	23.213	0.4308	4.0×10^{-4}
0.20	0.95	23.206	0.4309	8.0×10^{-4}
0.50	1.25	23.185	0.4313	2.0×10^{-3}

The mild sensitivity for a near 0.75 contrasts with the rapid deterioration of the Green kernel as the singular value $a = 16$ is approached. For reference, $\mathcal{K}_B(14) = 7.984$, $\mathcal{K}_B(15) = 4.405$, $\mathcal{K}_B(15.5) = 2.388$, and $\mathcal{K}_B(15.9) = 0.522$. For the fixed sharp Lipschitz constant $L = 10$, the equation $\mathcal{K}_B(a) = L$ has the numerical solution

$$a_{\text{crit}} \approx 13.4174.$$

Thus the contraction condition $L < \mathcal{K}_B(a)$ is valid only for $a < a_{\text{crit}}$. As $a \uparrow a_{\text{crit}}$ from below, $\tilde{q} = L/\mathcal{K}_B(a) \uparrow 1$ and the factor $(1 - \tilde{q})^{-1}$ diverges. For $a \geq a_{\text{crit}}$, Proposition 2 and the bound (43) no longer apply. Although D and E diverge as $a \to 16^-$, that singular limit lies outside the validity range of the contraction-based sensitivity estimate for the fixed value $L = 10$.

7.4. Benchmark Example: Green-Function Bounds and Admissible Lipschitz Constants

Consider the fractional boundary value problem

$$\begin{cases} D_t^{4.5} w(t) + \beta \dfrac{w(t)}{1 + \cosh(w(t))} + \cos\left(\dfrac{t}{4}\right) = 0, & t \in (0,1), \\ w(0) = w'(0) = w''(0) = w'''(0) = 0,\ w(1) = \dfrac{3}{4}\, w\left(\dfrac{1}{2}\right). \end{cases} \tag{44}$$

The nonlinear term is

$$h(t, w) = \beta \frac{w}{1 + \cosh(w)} + \cos\left(\frac{t}{4}\right). \tag{45}$$

In the benchmark analysis of Shivanian [7], the conservative Lipschitz constant $\mathcal{K} = \beta$ is used.

Since every numerical threshold below depends on this value, we verify it. Let $f(w) = w/(1 + \cosh w)$, so that $h(t, w) = \beta f(w) + \cos(t/4)$ and, by the mean value theorem, $|h(t, x) - h(t, y)| \leq \beta \sup_{w \in \mathbb{R}} |f'(w)|\, |x - y|$. Differentiating,

$$f'(w) = \frac{(1 + \cosh w) - w \sinh w}{(1 + \cosh w)^2}.$$

We claim that $|f'(w)| \leq \frac{1}{2}$ for every $w \in \mathbb{R}$, with equality at $w = 0$. For the upper bound, $f'(w) \leq \frac{1}{2}$ is equivalent to $\frac{1}{2}(1 + \cosh w)^2 - (1 + \cosh w) + w \sinh w \geq 0$; since

$\frac{1}{2}(1+\cosh w)^2 - (1+\cosh w) = \frac{1}{2}(1+\cosh w)(\cosh w - 1) = \frac{1}{2}(\cosh^2 w - 1) = \frac{1}{2}\sinh^2 w$, the left-hand side equals

$$\tfrac{1}{2}\sinh^2 w + w\sinh w = \sinh w\left(\tfrac{1}{2}\sinh w + w\right) \;\geq\; 0,$$

because both factors carry the sign of w. For the lower bound, $f'(w) \geq -\frac{1}{2}$ is equivalent to $(1+\cosh w) - w\sinh w + \frac{1}{2}(1+\cosh w)^2 \geq 0$; substituting $\cosh^2 w = 1 + \sinh^2 w$ and completing the square in $\sinh w$, the left-hand side equals

$$\tfrac{1}{2}(\sinh w - w)^2 + 2 + \left(2\cosh w - \tfrac{w^2}{2}\right) \;>\; 0,$$

because $2\cosh w \geq 2 + w^2 > \frac{w^2}{2}$. As $f'(0) = \frac{1}{2}$, we conclude that $\sup_{w\in\mathbb{R}} |f'(w)| = \frac{1}{2}$, so $h(t,\cdot)$ is globally Lipschitz with the *sharp* constant

$$L = \frac{\beta}{2}. \tag{46}$$

All three solvability criteria are therefore applied to L, not to β. Since each criterion requires the Lipschitz constant to be smaller than the corresponding admissible value, the conditions $L < \mathcal{K}_S$, $L < \mathcal{K}_B$ and $L < \mathcal{K}_B^*$ translate into the equivalent restrictions on the equation parameter β:

$$\beta < 2\mathcal{K}_S = 29.293, \qquad \beta < 2\mathcal{K}_B = 46.439, \qquad \beta < 2\mathcal{K}_B^* = 64.331. \tag{47}$$

We stress that this normalisation affects only the translation between L and β: the admissible constants $\mathcal{K}_S, \mathcal{K}_B, \mathcal{K}_B^*$ and the improvement factors R and R^* are properties of the Green function alone and are unchanged. (Shivanian [7] works with the conservative value $\mathcal{K} = \beta$; using the sharp constant $L = \beta/2$ is legitimate for all three criteria simultaneously and keeps the comparison fair.)

Moreover, the parameters of the problem are

$$\alpha = 4.5, \qquad c = 5, \qquad a = \frac{3}{4}, \qquad b = \frac{1}{2}. \tag{48}$$

Using Shivanian's criterion, the admissible Lipschitz constant is

$$\mathcal{K}_S = \frac{\Gamma(5.5)}{2\left(1 + \left|\frac{\frac{3}{4}}{1-\frac{3}{4}\left(\frac{1}{2}\right)^4}\right|\right)} = 14.646373600264974. \tag{49}$$

Hence Shivanian's theorem guarantees existence and uniqueness whenever

$$L < 14.646373600264974, \qquad \text{equivalently} \qquad \beta < 29.29274720052995. \tag{50}$$

For the proposed criterion, we compute

$$D = \frac{1}{1-\frac{3}{4}\left(\frac{1}{2}\right)^4} = 1.0491803279, \text{ and } E = \frac{\frac{3}{4}}{1-\frac{3}{4}\left(\frac{1}{2}\right)^4} = 0.7868852459. \tag{51}$$

Since $n = \alpha - 1 = 3.5$, we obtain

$$|E|\, b^n - D = 0.7868852459\left(\frac{1}{2}\right)^{3.5} - 1.0491803279 = -0.9796288 < 0. \tag{52}$$

Therefore,

$$\max\left\{0, \frac{2(|E|b^n - D)}{n+1}\right\} = 0. \tag{53}$$

Consequently, $\mathcal{K}_B = 23.220$. Thus existence and uniqueness are guaranteed whenever

$$L < 23.21950343808252, \qquad \text{equivalently} \qquad \beta < 46.43900687616504. \tag{54}$$

Comparing the two admissible constants,

$$\mathcal{K}_S = 14.646, \qquad \mathcal{K}_B = 23.220, \tag{55}$$

and therefore

$$R = \frac{\mathcal{K}_B}{\mathcal{K}_S} = 1.585. \tag{56}$$

This means that the proposed criterion allows a Lipschitz constant approximately 58.5% larger than that permitted by Shivanian's theorem.

We now apply the refined criterion of Corollary 2. Here

$$\delta = D - |E|b^n = 1.0491803279 - 0.7868852459\left(\frac{1}{2}\right)^{3.5} = 0.9796288 > 0, \tag{57}$$

so the corollary is applicable; note that $\delta = -\big(|E|b^n - D\big)$, so this is the same quantity as in (52), with the opposite sign. With $m = 4$ and $n = 3.5$,

$$\tau = \frac{2n+1}{2(m+2n+1)\delta} = \frac{8}{24 \times 0.9796288} = 0.3402649 < 1, \tag{58}$$

and therefore

$$G(\delta) = \frac{m\,\tau^{(2n+1)/m}}{(m+2n+1)(2n+1)} = \frac{4\,\tau^2}{96} = 0.0048242, \qquad Q(b,n) + G(\delta) = 0.1307715. \tag{59}$$

Consequently,

$$\mathcal{K}_B^* = \frac{\Gamma(4.5)}{\sqrt{0.1307715}} = 32.165, \tag{60}$$

which further improves the constant $\mathcal{K}_B = 23.220$ of Theorem 2 and yields the improvement factor

$$R^* = \frac{\mathcal{K}_B^*}{\mathcal{K}_S} = \frac{32.165}{14.646} = 2.196. \tag{61}$$

Figure 2 displays, for the benchmark parameters (48), the exact function $I(t)$ computed by adaptive numerical quadrature of (15), together with the pointwise bound of Theorem 1, the refined pointwise bound $\Phi(t)$ of Proposition 1, and the two global bounds $Q(b,n) + \frac{1}{2n+1}$ and $Q(b,n) + G(\delta)$. The figure illustrates the strict hierarchy

$$I(t) \;\le\; \Phi(t) \;\le\; Q(b,n)t^{2m} + \frac{t^{2n+1}}{2n+1}, \qquad t \in (0,1),$$

established in Proposition 1, and shows that retaining the negative mixed term reduces the pointwise estimate by more than an order of magnitude over most of the interval. Figure 2 thus serves as a direct numerical verification of the theoretical Green-function estimates: the exact $I(t)$ is evaluated by adaptive quadrature of the decomposition (15) (with the closed forms of Lemma 1 cross-checked against direct quadrature of the definition (13) to machine precision), and the computed curve lies below the pointwise bound of Theorem 1 and below $\Phi(t)$ at every sample point, as the theory predicts. The figure also illustrates Remark 6: a direct numerical maximisation of Φ gives

$$\sup_{0<t<1} \Phi(t) = \Phi(1) = Q(b,n) + \frac{1-2\delta}{2n+1} = 6.0402 \times 10^{-3},$$

which corresponds to the admissible constant $\Gamma(4.5)/\sqrt{6.0402 \times 10^{-3}} \approx 149.66$, that is, more than ten times Shivanian's constant. This confirms that the closed-form criterion of Corollary 2, although already a strict improvement, is itself conservative, the loss originating in the bound $Q(b,n)t^{2m} \leq Q(b,n)$ used in the proof of Corollary 1.

To illustrate the practical significance of this improvement we use the equivalent parameter ranges (47). Consider $\beta = 40$, for which the sharp Lipschitz constant is $L = 20$. Since $20 > \mathcal{K}_S = 14.646$, Shivanian's theorem is not applicable; however $20 < \mathcal{K}_B = 23.220$, so existence and uniqueness still follow from Theorem 2. For $\beta = 60$ one has $L = 30$, and neither Shivanian's criterion nor Theorem 2 applies, since $30 > 23.220$; nevertheless $30 < \mathcal{K}_B^* = 32.165$, and existence and uniqueness follow from Corollary 2. Equivalently, in terms of the equation parameter, the three criteria certify the benchmark problem for $\beta < 29.293$, $\beta < 46.439$ and $\beta < 64.331$, respectively. These examples demonstrate the advantage of the improved Green-function estimates.

7.5. Additional Numerical Comparisons Across Parameter Configurations

We now compare the admissible Lipschitz constants

$$\mathcal{K}_S = \frac{\Gamma(\alpha+1)}{2(1+|E|)} \tag{62}$$

and

$$\mathcal{K}_B = \frac{\Gamma(\alpha)}{\sqrt{Q(b,n) + \dfrac{1}{2n+1} + \max\left\{0, \dfrac{2(|E|b^n - D)}{n+1}\right\}}}. \tag{63}$$

For convenience, we introduce the improvement factor

$$R = \frac{\mathcal{K}_B}{\mathcal{K}_S}. \tag{64}$$

Values of $R > 1$ indicate that the proposed criterion is less restrictive than Shivanian's criterion. In the regime $|E|b^n \leq D$, that is, $\delta = D - |E|b^n \geq 0$, we also report the refined constant $\mathcal{K}_B^*$ of Corollary 2 and the corresponding improvement factor

$$R^* = \frac{\mathcal{K}_B^*}{\mathcal{K}_S}. \tag{65}$$

When $\delta < 0$, Corollary 2 does not apply and Theorem 2 remains the operative criterion; the corresponding entries are marked with a dash.

Table 5 shows that the proposed criterion consistently yields a larger admissible Lipschitz constant than Shivanian's criterion for all tested parameter configurations, and that the refined criterion of Corollary 2 provides a further strict improvement whenever it applies.

Table 5. Comparison between Shivanian's criterion, the proposed criterion of Theorem 2, and the refined criterion of Corollary 2.

α	c	a	b	$\mathcal{K}_S$	$\mathcal{K}_B$	R	δ	$\mathcal{K}_B^*$	R^*
3.0	3	0.75	0.50	1.560	3.033	1.944	1.0000	4.089	2.621
4.5	5	0.75	0.50	14.646	23.220	1.585	0.9796	32.165	2.196
4.5	5	0.75	0.75	13.196	23.199	1.758	0.9519	32.076	2.431
4.5	5	15.00	0.50	0.109	4.405	40.561	<0	—	—
4.5	5	32.00	0.50	0.793	8.249	10.402	<0	—	—
3.0	3	1.00	0.90	0.479	2.782	5.809	1.0000	3.530	7.369

In particular, the improvement becomes more pronounced when $|1 - ab^{c-1}|$ approaches zero, corresponding to parameter values close to the singular regime of the boundary condition. Two distinct situations must nevertheless be distinguished, since a large improvement factor does not by itself indicate proximity to the singular set. The configuration $\alpha = 4.5$, $c = 5$, $a = 15$, $b = \frac{1}{2}$ gives $ab^{c-1} = 15/16$ and $|1 - ab^{c-1}| = 1/16$: it approaches the singular value $a = 16$ from *within* the region $ab^{c-1} < 1$, where $D = 16 > 0$ and $E = 240$, and the large factor $R = 40.561$ recorded in Table 5 is genuinely driven by proximity to the singular set. By contrast, the configuration $a = 32$, $b = \frac{1}{2}$ gives $ab^{c-1} = 2$, hence $1 - ab^{c-1} = -1$ and $|1 - ab^{c-1}| = 1$: this configuration is not close to the singular set at all, but lies on the *opposite side* of it, where $D = -1 < 0$ and $E = -32$. The factor $R = 10.402$ observed there therefore reflects the change of sign regime in D and E rather than proximity to $ab^{c-1} = 1$. In both configurations $\delta < 0$, so Corollary 2 does not apply and Theorem 2 remains the operative criterion. Proximity to the singular set and location on its far side are thus distinct effects and should not be conflated.

Remark 14. *When $\alpha = c$, one has $n = m$, and if in addition $a > 0$ and $1 - ab^m > 0$, then*

$$\delta = D - |E|b^n = D - aDb^m = D\,(1 - ab^m) = 1.$$

This explains the two entries $\delta = 1$ in Table 5.

The data of Table 5 are visualized in Figure 3, which compares the three admissible Lipschitz constants on a logarithmic scale. The figure makes apparent the systematic gain of $\mathcal{K}_B$ over $\mathcal{K}_S$. The two largest gains occur for the configurations $a = 15$ and $a = 32$, but for different reasons: the first is genuinely close to the singular set, whereas the second lies in the opposite-sign regime $1 - ab^{c-1} < 0$. The figure also displays the further gain of $\mathcal{K}_B^*$ over $\mathcal{K}_B$ whenever $\delta \geq 0$.

Finally, Figure 4 examines the dependence of the improvement factors on the boundary parameter a. We fix $\alpha = 4.5$, $c = 5$, $b = \frac{1}{2}$, and let a range over $(0, 16)$, the right endpoint corresponding to the singular regime $ab^{c-1} = 1$. Three features are visible. First, $R > 1$ for every a in the range considered, so the proposed criterion is uniformly less restrictive than Shivanian's in this family. Second, $R^* \geq R$ on the subinterval $0 < a \leq 2^{3.5} \approx 11.314$ where $\delta \geq 0$, and the two curves merge exactly at $\delta = 0$, consistently with the fact that $G(0) = \frac{1}{2n+1}$, in which case the criteria of Theorem 2 and Corollary 2 coincide. Third, R grows without bound as a approaches the singular value $a = 16$, quantifying the observation that the improvement is most significant near the singular regime of the boundary condition.

Remark 15 (Computational cost of the refined constants)**.** *Evaluating the proposed constants is essentially free. The constant $\mathcal{K}_B$ of (30) requires the elementary quantities D, E, one evaluation of $\Gamma(\alpha)$, and one evaluation of the Gauss hypergeometric value ${}_2F_1(-n,1;n+2;b)$ entering $Q(b,n)$; since $0 < b < 1$, the defining hypergeometric series converges geometrically and is available in every standard special-function library, so the constant requires only a fixed, small number of elementary and special-function evaluations.*

More precisely, evaluating $\mathcal{K}_B$ requires one evaluation of $\Gamma(\alpha)$ and one of ${}_2F_1(-n,1;n+2;b)$, together with a fixed number of elementary operations. The cost of each special-function evaluation to a prescribed accuracy depends on the requested precision and on the library implementation. At standard double precision, these evaluations are inexpensive relative to the quadrature and optimisation steps used in the numerical illustrations.

The refined constant $\mathcal{K}_B^*$ of (28) adds only the closed-form quantities δ, τ and $G(\delta)$, i.e., a few additional elementary operations. Even the sharpest variant of Remark 6, the numerical maximisation of the explicit scalar function Φ on $[0,1]$, is only a one-dimensional optimisation of a smooth function. All reported constants were computed in double precision and independently verified using 40-digit arithmetic $(\texttt{mp.dps} = 40)$ and adaptive quadrature.

These numerical results confirm that the refined Green-function estimate captures additional information that is not reflected in the classical $\mathbf{L}^1$-based analysis. Consequently, the resulting Banach-type criterion applies to a substantially broader class of nonlinear fractional boundary value problems.

7.6. Convergence of the Fixed-Point Iteration

The comparisons above are computations of admissible *constants*. We now report a genuine numerical experiment, namely the Picard iteration

$$u_{k+1} = Tu_k, \qquad u_0 \equiv 0,$$

associated with the benchmark problem (44), discretised as described in the reproducibility paragraph of Section 7. Figure 5 plots $\|u_k - u_{k-1}\|_\infty$ against k on a logarithmic scale for $\beta = 28, 40, 60$ (equivalently, for the sharp Lipschitz constants $L = \beta/2 = 14, 20, 30$), and Table 6 reports the certified contraction factors, the number of iterations required to reach the tolerance 10^{-6}, the empirical convergence factor, and the median solve time.

The experiment must be read with one point of principle in mind. Convergence of the iteration is governed by whether T is an *actual* contraction, not by which sufficient criterion happens to be satisfied; the failure of a sufficient condition does not by itself cause the iteration to diverge. For the benchmark parameters (48) the numerically estimated kernel norm is

$$\sup_{0<t<1} \int_0^1 |\mathbf{Gr}(t,s)|\, ds \;\approx\; 1.4113 \times 10^{-3},$$

obtained by finite quadrature on the grid described above and stable to approximately five significant digits under refinement from $N = 301$ to $N = 4801$. This value lies substantially below all the closed-form bounds derived here; accordingly the iteration converges geometrically and reaches 10^{-6} within three iterations for all three values of β, the empirical convergence factor (the median ratio of successive differences along the computed trajectory) being at most 7.6×10^{-3}. We emphasise that this quantity is an observed ratio along a single Picard trajectory, not the exact Lipschitz modulus of T.

Two conclusions should be drawn carefully. First, since all three cases reach the tolerance in the same number of iterations, the experiment does *not* show that the refined bound makes the iteration converge faster; the observed rate is governed by the actual nonlinear operator. The Green kernel is common to all three cases, whereas the nonlinear scaling varies with β. What the experiment does show is that the refined bounds provide *stronger a priori certification*: for $\beta = 40$ ($L = 20$) Shivanian's criterion gives $q_S = 1.366 \geq 1$ and certifies nothing, whereas $\mathcal{K}_B$ and $\mathcal{K}_B^*$ both certify a contraction; for $\beta = 60$ ($L = 30$) even $q_B = 1.292 \geq 1$, and only Corollary 2, with $q^* = 0.933 < 1$, certifies the result. Second, the convergence observed in precisely those cases confirms quantitatively that all three criteria remain conservative, as anticipated in Remarks 3 and 6.

Table 6. Certified versus observed contraction data for the benchmark problem (44) with the parameters (48). All criteria are applied to the sharp Lipschitz constant $L = \beta/2$ of (46). A dagger (†) marks a certified factor ≥ 1, i.e., a criterion that does not guarantee a contraction. The iteration nevertheless converges in every case, the empirical convergence factor being far below each a priori bound. Timings are the median of 100 repeated solves after precomputation of the discrete Green matrix, with the interquartile range in parentheses.

β	$L = \beta/2$	$q_S = L/\mathcal{K}_S$	$q_B = L/\mathcal{K}_B$	$q^* = L/\mathcal{K}_B^*$	Iterations to 10^{-6}	Empirical Factor	Median Time (ms)
28	14	0.956	0.603	0.435	3	3.5×10^{-3}	1.54 (0.07)
40	20	1.366 †	0.861	0.622	3	5.1×10^{-3}	1.53 (0.09)
60	30	2.048 †	1.292 †	0.933	3	7.6×10^{-3}	1.51 (0.06)

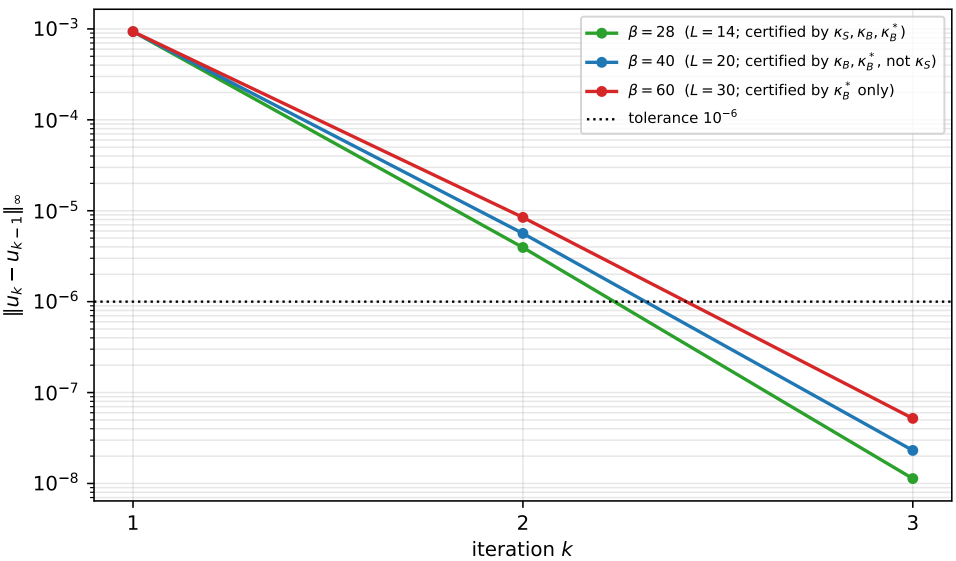

Figure 5. Convergence of the fixed-point iteration $u_{k+1} = Tu_k$, $u_0 \equiv 0$, for the benchmark problem (44) with $\beta = 28, 40, 60$, i.e., with sharp Lipschitz constants $L = \beta/2 = 14, 20, 30$. The iteration converges geometrically in all three cases and reaches the tolerance 10^{-6} within three iterations. The empirical convergence factors are substantially smaller than the certified bounds and are of the same order of magnitude in the three cases, reflecting the conservativeness of the a priori estimates rather than any speed-up due to the refined bounds.

8. Conclusions

This paper has developed a unified framework for the Caputo fractional three-point boundary value problem (1), resting on a single refined pointwise $\mathbf{L}^2$ estimate for the associated Green function. Three distinct contributions emerge from this estimate.

Sharper existence and uniqueness. The new bound for $\sup_{0<t<1}\int_0^1 \mathbf{Gr}^2(t,s)\,ds$ retains a negative mixed term discarded in the $\mathbf{L}^1$ analysis of Shivanian [7], yielding an improved admissible Lipschitz constant $\mathcal{K}_B > \mathcal{K}_S$ in an explicit parameter regime, and a further closed-form refinement $\mathcal{K}_B^* \geq \mathcal{K}_B$. A comparison theorem identifies the conditions under which the improvement is operative; the gain is most pronounced near the singular regime $ab^{c-1} = 1$. Applied to Shivanian's benchmark, the admissible constant rises from 14.646 to 23.220 (factor 1.585) and then to 32.165 (factor 2.196).

Ulam–Hyers stability. The contraction constant furnished by the refined $\mathbf{L}^2$ estimate is directly used to establish that every solution of (1) is Ulam–Hyers stable with the explicit stability constant $C_{\mathrm{UH}} = (1-q)^{-1}$ (Theorem 4). A Ulam–Hyers estimate already follows from the classical $\mathbf{L}^1$ contraction condition whenever $q_S < 1$; the contribution here is quantitative: the refined constant enlarges the range of $\mathcal{K}$ for which stability is certified and yields a strictly smaller stability constant than the coarser $\mathbf{L}^1$ bound.

Continuous dependence on data. The same contraction framework yields explicit quantitative bounds on the sensitivity of the unique solution to perturbations in the nonlinearity h (Theorem 5) and in the boundary parameter a (Proposition 2). Both bounds are tighter under the refined $\mathbf{L}^2$ estimate than under the classical $\mathbf{L}^1$ approach, because the refined estimate produces a smaller contraction constant. The analysis also characterizes the deterioration of the Green kernel and of the contraction-based sensitivity estimate as the boundary parameters approach resonance. For a fixed Lipschitz constant, the estimate becomes singular as the perturbed contraction factor approaches one and ceases to apply once the contraction condition fails.

Overall, the results show that a more accurate analysis of the Green function simultaneously sharpens solvability conditions, stability estimates, and sensitivity bounds.

Limitations. The framework has clear boundaries that should be stated explicitly. First, all criteria in this paper are *sufficient* conditions: a nonlinearity violating $\mathcal{K} < \mathcal{K}_B^*$ may still yield a unique solution, and none of our bounds is claimed to be attained (Remark 6). Second, the main results assume a *global* Lipschitz condition; the relaxation to local Lipschitz or φ-contraction conditions sketched in Remark 5 yields only local uniqueness and was not developed in full. Third, the closed-form refinement of Corollary 2 is restricted to the regime $\delta \geq 0$ and is conservative within it (Remark 3). Fourth, the analysis is confined to a scalar problem on $[0,1]$ with a single interior node; and near the singular regime $ab^{c-1} = 1$ every criterion, old or new, degenerates, as quantified in Section 7.3.

Future directions. The refined Green-function programme suggests several concrete continuations. (i) *Multipoint and higher-order problems:* the decomposition of Lemma 2 extends structurally to m-point conditions $u(1) = \sum_{i=1}^{k} a_i\,u(b_i)$, at the cost of a matrix of mixed terms I_{ij} whose sign analysis parallels Theorem 1; higher-order nonlocal conditions involving derivatives at the nodes appear equally tractable. (ii) *Other fractional operators:* for the Caputo–Fabrizio and Atangana–Baleanu derivatives the associated kernels are nonsingular (exponential and Mittag–Leffler, respectively), so the analogue of $I(t)$ is again an explicit double integral and the same $\mathbf{L}^2$/Cauchy–Schwarz strategy—retain the sign-definite mixed term rather than discard it—is expected to sharpen existing contraction criteria; the tempered Caputo setting of [31] is a natural first test case. (iii) *Systems:* extending the estimates to coupled systems requires vector-valued Green matrices and Perov-type contraction arguments. (iv) *Optimal constants:* closing the gap between $\mathcal{K}_B^*$ and the constant obtained from the exact $\sup_{0<t<1}\Phi(t)$ (Remark 3), and ultimately from $\sup_{0<t<1}\int_0^1 \mathbf{Gr}^2(t,s)\,ds$ itself, is an open analytic problem.

Adaptive Fourier decomposition in Hardy spaces [38,39], which produces optimal rational approximations of a given kernel, appears to be a promising tool for this purpose: it would replace the elementary majorisation $(b-s)^n \le b^n(1-s)^n$ used in the proof of Theorem 1 by an adaptive expansion of $\mathbf{Gr}(t,\cdot)$, and may thereby provide alternative approximations or bounds with less slack than the elementary majorisation used here. Whether such an approach attains the exact supremum in the present setting is an open question, which we do not claim to settle.

(v) *Two-metric approaches:* combining the present estimates with Rus's fixed-point theorem [23] in the spirit of [20,22] may enlarge the admissible class further and will be pursued elsewhere.

(vi) *Fractal and stochastic models of oscillatory and wave phenomena:* recent work in the fractals literature continues to generate fractional and fractal formulations of concrete nonlinear systems; two representative examples are the fractal stochastic model of ion sound and Langmuir waves analysed in [40] and the fractional rotating pendulum oscillator investigated numerically in [41]. Such models are typically treated by approximate analytical or numerical techniques—harmonic balance, homotopy perturbation, frequency formulations—whose meaningful application presupposes that the underlying fractional problem is well posed; contraction frameworks with explicit constants, of the type sharpened in this paper, supply exactly this foundation, certifying existence and uniqueness and quantifying the sensitivity of the solution to perturbations of the data. In particular, the explicit Ulam–Hyers estimate of Theorem 4 offers a deterministic template for stability statements under stochastic perturbations of the kind arising in [40], and transporting the present programme—retain, rather than discard, the sign-definite mixed term in the kernel estimate—to the integral kernels associated with fractional oscillator and wave models, including their fractal and stochastic variants, appears to be a natural continuation of the directions listed above.

Supplementary Materials: The following supporting information can be downloaded at https://www.mdpi.com/article/10.3390/math14152840/s1, Complete Python script.

Funding: This research was funded by the Deanship of Graduate Studies and Scientific Research at Qassim University, grant number QU-APC-2026.

Data Availability Statement: No new data were created or analyzed in this study. Data sharing is not applicable to this article.

Acknowledgments: The Researchers would like to thank the Deanship of Graduate Studies and Scientific Research at Qassim University (https://www.qu.edu.sa) for financial support (QU-APC-2026).

Conflicts of Interest: The author declares no conflicts of interest.

References

1. Hilfer, R. (Ed.) *Applications of Fractional Calculus in Physics*; World Scientific: Singapore, 2000.
2. Magin, R.L. *Fractional Calculus in Bioengineering*; Begell House: Redding, CT, USA, 2006.
3. Ionescu, C.; Lopes, A.; Copot, D.; Machado, J.A.T.; Bates, J.H.T. The role of fractional calculus in modeling biological phenomena: A review. *Commun. Nonlinear Sci. Numer. Simul.* **2017**, *51*, 141–159. [CrossRef]
4. Mainardi, F. *Fractional Calculus and Waves in Linear Viscoelasticity: An Introduction to Mathematical Models*; Imperial College Press: London, UK, 2010.
5. Sun, H.; Zhang, Y.; Baleanu, D.; Chen, W.; Chen, Y. A new collection of real world applications of fractional calculus in science and engineering. *Commun. Nonlinear Sci. Numer. Simul.* **2018**, *64*, 213–231. [CrossRef]
6. Liu, Y.; Wang, X.; Zhuang, L.; Stapleton, M.; Zhang, H. Increasing biosensor-based cell selection pressure improves microbial biosynthesis of 4-hydroxybenzoate. *Biochem. Eng. J.* **2024**, *205*, 109265. [CrossRef]

7. Shivanian, E. On the solution of Caputo fractional high-order three-point boundary value problem with applications to optimal control. *J. Nonlinear Math. Phys.* **2024**, *31*, 2. [CrossRef]
8. Podlubny, I. *Fractional Differential Equations*; Academic Press: San Diego, CA, USA, 1999.
9. Kilbas, A.A.; Srivastava, H.M.; Trujillo, J.J. *Theory and Applications of Fractional Differential Equations*; Elsevier: Amsterdam, The Netherlands, 2006.
10. Diethelm, K. *The Analysis of Fractional Differential Equations*; Springer: Berlin, Germany, 2010.
11. Il'in, V.A.; Moiseev, E.I. Nonlocal boundary value problem of the first kind for a Sturm–Liouville operator in its differential and finite difference aspects. *Differ. Equ.* **1987**, *23*, 803–810.
12. Gupta, C.P. Solvability of a three-point nonlinear boundary value problem for a second order ordinary differential equation. *J. Math. Anal. Appl.* **1992**, *168*, 540–551. [CrossRef]
13. Bai, Z.; Lü, H. Positive solutions for boundary value problem of nonlinear fractional differential equation. *J. Math. Anal. Appl.* **2005**, *311*, 495–505. [CrossRef]
14. Liang, S.; Zhang, J. Positive solutions for boundary value problems of nonlinear fractional differential equation. *Nonlinear Anal. Theory Methods Appl.* **2009**, *71*, 5545–5550. [CrossRef]
15. Li, C.F.; Luo, X.N.; Zhou, Y. Existence of positive solutions of the boundary value problem for nonlinear fractional differential equations. *Comput. Math. Appl.* **2010**, *59*, 1363–1375. [CrossRef]
16. Agarwal, R.P.; Benchohra, M.; Hamani, S. A survey on existence results for boundary value problems of nonlinear fractional differential equations and inclusions. *Acta Appl. Math.* **2010**, *109*, 973–1033. [CrossRef]
17. Chai, G.; Hu, S. Existence of positive solutions for a fractional high-order three-point boundary value problem. *Adv. Differ. Equ.* **2014**, *2014*, 90. [CrossRef]
18. Banach, S. Sur les opérations dans les ensembles abstraits et leur application aux équations intégrales. *Fundam. Math.* **1922**, *3*, 133–181. [CrossRef]
19. Smirnov, S. Green's function and existence of solutions for a third-order three-point boundary value problem. *Math. Model. Anal.* **2019**, *24*, 171–178. [CrossRef]
20. Almuthaybiri, S.S.; Tisdell, C.C. Sharper existence and uniqueness results for solutions to third-order boundary value problems. *Math. Model. Anal.* **2020**, *25*, 409–420. [CrossRef]
21. Almuthaybiri, S.S.; Tisdell, C.C. Existence and uniqueness of solutions to third-order boundary value problems: Analysis in closed and bounded sets. *Differ. Equ. Appl.* **2020**, *12*, 291–312. [CrossRef]
22. Almuthaybiri, S.S.; Tisdell, C.C. Sharper existence and uniqueness results for solutions to fourth-order boundary value problems and elastic beam analysis. *Open Math.* **2020**, *18*, 1006–1024. [CrossRef]
23. Rus, I.A. On a fixed point theorem of Maia. *Stud. Univ. Babeş–Bolyai Math.* **1977**, *22*, 40–42.
24. Ulam, S.M. *A Collection of Mathematical Problems*; Interscience Publishers: New York, NY, USA, 1960.
25. Hyers, D.H. On the stability of the linear functional equation. *Proc. Natl. Acad. Sci. USA* **1941**, *27*, 222–224. [CrossRef] [PubMed]
26. Wang, J.; Lv, L.; Zhou, Y. Ulam stability and data dependence for fractional differential equations with Caputo derivative. *Electron. J. Qual. Theory Differ. Equ.* **2011**, *63*, 1–10. [CrossRef]
27. Benchohra, M.; Lazreg, J.E. Existence and Ulam stability for nonlinear implicit fractional differential equations with Hadamard derivative. *Stud. Univ. Babeş–Bolyai Math.* **2017**, *62*, 27–38. [CrossRef]
28. Rus, I.A. Ulam stabilities of ordinary differential equations in a Banach space. *Carpathian J. Math.* **2010**, *26*, 103–107.
29. da C. Sousa, J.V.; de Oliveira, E.C. Ulam–Hyers stability of a nonlinear fractional Volterra integro-differential equation. *Appl. Math. Lett.* **2018**, *81*, 50–56. [CrossRef]
30. Ran, C.; Xu, X.; Hou, C.; Zhang, X. Numerical approximation of fourth-order fractional diffusion-wave systems using finite difference and discontinuous Galerkin method. *Netw. Heterog. Media* **2025**, *20*, 1346–1366. [CrossRef]
31. Feruk, V. Boundary-value problem for a system of fractional differential equations with tempered Caputo derivative. *J. Math. Anal. Appl.* **2026**, *558*, 130455. [CrossRef]
32. Song, Z.; Jiang, Z. MP-FVM: Enhancing finite volume method for water infiltration modeling in unsaturated soils via message-passing encoder–decoder network. *Comput. Geotech.* **2026**, *190*, 107745. [CrossRef]
33. Song, Z.; Jiang, Z. A physics-based, data-driven numerical framework for anomalous diffusion of water in soil. *Syst. Control Trans.* **2025**, *4*, 2391–2397. [CrossRef]
34. Tian, D.; Ain, Q.-T.; Anjum, N.; He, C.-H.; Cheng, B. Fractal N/MEMS: From pull-in instability to pull-in stability. *Fractals* **2021**, *29*, 2150030. [CrossRef]
35. Demir, E.; Ozkol, I. Fractional-based nonlinear mechanical system modeling with FELEs: Numerical analysis of oscillatory and nonoscillatory behavior of the inverted pendulum system. *Arch. Appl. Mech.* **2025**, *95*, 152. [CrossRef]
36. Macías-Díaz, J.E.; Bountis, T. An efficient dissipation-preserving numerical scheme to solve a Caputo–Riesz time-space-fractional nonlinear wave equation. *Fractal Fract.* **2022**, *6*, 500. [CrossRef]

37. List, F.; Radu, F.A. A study on iterative methods for solving Richards' equation. *Comput. Geosci.* **2016**, *20*, 341–353. [CrossRef]
38. Qian, T. Intrinsic mono-component decomposition of functions: An advance of Fourier theory. *Math. Methods Appl. Sci.* **2010**, *33*, 880–891. [CrossRef]
39. Song, Z.; Sun, Z. Representing functions in H^2 on the Kepler manifold via WPOAFD based on the rational approximation of holomorphic functions. *Mathematics* **2022**, *10*, 2729. [CrossRef]
40. Lu, J.; Jin, L.; Xu, X.; Jiang, D.; He, D. Analysis of a fractal stochastic ion sound and Langmuir waves model. *Fractals* **2026**, 2650120. [CrossRef]
41. Jin, L.; Shen, S.-W.; Lu, J.; Chen, L.; Li, S.-H. Numerical analysis of a fractional rotating pendulum oscillator. *Fractals* **2026**, *34*, 2650064. [CrossRef]